

# Spring temperature responses of oaks are synchronous with North Atlantic conditions during the last deglaciation

STEVEN L. VOELKER,<sup>1,5</sup> PAUL-EMILE NOIROT-COSSON,<sup>2</sup> MICHAEL C. STAMBAUGH,<sup>3</sup> ERIN R. McMURRY,<sup>3</sup>  
FREDERICK C. MEINZER,<sup>4</sup> BARBARA LACHENBRUCH,<sup>2</sup> AND RICHARD P. GUYETTE<sup>3</sup>

<sup>1</sup>*Southern Oregon University, Biology Department, 1250 Siskiyou Boulevard, Ashland, Oregon 97520 USA*

<sup>2</sup>*Oregon State University, Department of Wood Science and Engineering, Corvallis, Oregon 97330 USA*

<sup>3</sup>*University of Missouri, Department of Forestry, 203ABNR Building, Columbia, Missouri 65211 USA*

<sup>4</sup>*USDA Forest Service, Forest Sciences Laboratory, 3200 Jefferson Way, Corvallis, Oregon 97330 USA*

**Abstract.** Paleoclimate proxies based on the measurement of xylem cell anatomy have rarely been developed across the temperature range of a species or applied to wood predating the most recent millennium. Here we describe wood anatomy-based proxies for spring temperatures in central North America from modern bur oaks (*Quercus macrocarpa* Michx.). The strong coherence of temperature signals across the species range supports the use of these proxies across thousands of years of climatic change. We also used 79 subfossil oak log cross sections from northern Missouri, <sup>14</sup>C-dated to 9.9–13.63 ka (ka is 1000 cal yr BP), to assess the frequency of oak deposition into alluvial sediments and a subset of these oaks for a wood anatomy-based reconstruction of spring paleotemperatures. Temperatures during the Younger Dryas cold period (YD) were up to 3.5°C lower than modern temperatures for that region, equivalent to or lower than those experienced at the northern edge of the modern species range. Compared to extant oaks growing at much higher [CO<sub>2</sub>], subfossil oaks had greater vessel frequencies. Besides very low theoretical (or estimated) xylem conductivity near the beginning of the oak record near 13.6 ka, vessel frequencies greater than modern trees compensated for reduced vessel dimensions so that theoretical xylem conductivity was consistently above that of modern trees at the cold northern sites. Significant correlations were found between the frequency of <sup>14</sup>C-dated oaks and either δ<sup>18</sup>O from the NGRIP (North Greenland Ice Core Project) ice core or from the Cariaco grayscale marine-sediment record from the southern Caribbean sea. Oak deposition into alluvial sediments during the YD was significantly lower than expected given the average sample depth of oaks from 9.9 to 13.6 ka. Reduced oak deposition during the YD suggests that an abrupt shift in climate reduced oak populations across the region and/or changed the rates of channel movement across drainages.

**Key words:** *Bølling-Allerød; bur oak; Great Plains, USA; Holocene; phenology; Pleistocene; Pre-Boreal; Quercus macrocarpa; radiocarbon; wood anatomy; xylem; Younger Dryas.*

## INTRODUCTION

Late Quaternary warming in the North Atlantic region underwent a rapid and iconic reversal in temperatures known as the Younger Dryas cold event (YD; 12.9–11.6 ka, ka is 1000 cal yr BP) that has been linked with a near cessation in the North Atlantic ocean meridional overturning (Jouzel et al. 1997, Alley 2000, Carlson et al. 2007, Carlson 2010). Reductions in ocean cycling and associated changes in atmospheric circulation influenced temperatures throughout the Northern Hemisphere (Mikolajewicz et al. 1997, Peteet et al. 1997). Indeed, even tropical latitudes were affected by changes in trade wind flow during the YD (Hughen et al. 1996, 2000).

Extensive pollen data from the late Quaternary show abrupt changes in vegetation across eastern North America synchronous with the North Atlantic Stratig-

raphy (Shane and Anderson 1993, Shuman et al. 2002, Williams et al. 2004, Viau et al. 2006, Gonzales and Grimm 2009). A review of paleoclimate data led Yu and Wright (2001) to infer that shifts in atmospheric circulation patterns propagated across mid-continental North America but the mechanisms, timing, and extent of these effects remain uncertain. More recent proxy evidence from the American mid-continent has shed light on the timing and complexity of vegetation dynamics over the Great Plains and Midwest during the late Quaternary, but evidence has still been elusive for widespread changes in temperature, its seasonality, and associated patterns in wetness or aridity during the YD (Denniston et al. 2001, Haynes 2008, Nordt et al. 2008, Gill et al. 2009, Gonzales and Grimm 2009, Dorale et al. 2010, Saunders et al. 2010).

Strong efforts in Europe to collect buried subfossil wood have produced tree-ring chronologies that extend across the Holocene and into the late glacial period (Becker 1993, Kromer and Spurk 1998, Spurk et al.

Manuscript received 10 May 2011; revised 25 August 2011; accepted 27 September 2011. Corresponding Editor: F. S. Hu.

<sup>5</sup> E-mail: voelkerst@sou.edu

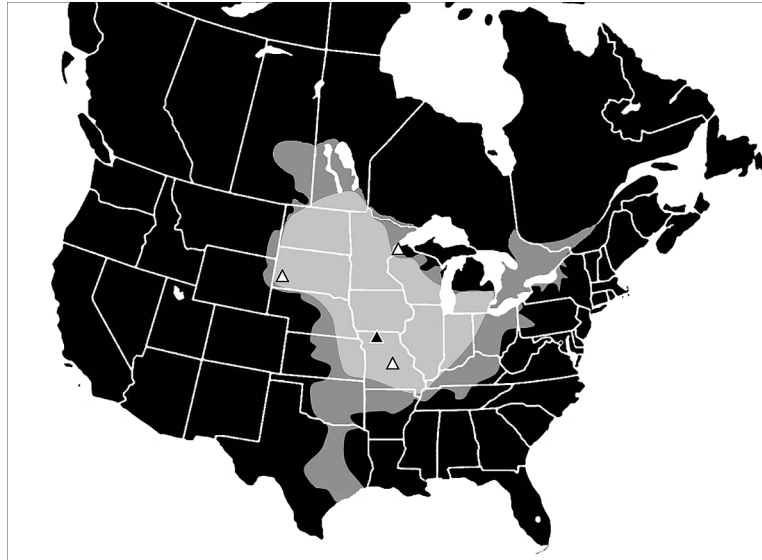


FIG. 1. Locations of sampling areas for modern oaks in central Missouri (MO), Wisconsin (WI), and South Dakota (SD), USA, are indicated by open triangles, and the subfossil oak collection area in northern Missouri is indicated by a solid triangle. The bur oak (*Quercus macrocarpa*) range is approximated in dark gray (adapted from Burns and Honkala [1990]), while the light gray shading indicates the approximated core range, where USDA Forest Service inventory data indicate it grows as a frequent component of riparian and some upland forests.

2002, Friedrich et al. 2004). In North America these ends have rarely been pursued outside of bristlecone pine (*Pinus longaeva* D.K. Bailey) remnants preserved at high elevation. At present we have a collection of nearly 400 subfossil bur oak (*Quercus macrocarpa* Michx.) and swamp white oak (*Q. bicolor* Willd.) stem cross sections from northern Missouri, USA that have been  $^{14}\text{C}$ -dated to 13.84 ka in age (Guyette et al. 2008, Stambaugh and Guyette 2009). These species co-occur across most of our Missouri sample region and cannot be differentiated by their wood anatomy. Swamp white oak is only a minor component of modern forests that occur on poorly drained soils, and this species has a restricted latitudinal range compared to bur oak (Burns and Honkala 1990). Therefore the rest of the paper shall focus on bur oak. Subfossil oaks fell into streams and were deposited in alluvial sediments long ago and were collected within the last decade after being reexposed by stream channel movement. Interannual variation in tree-ring variables has been used to reconstruct late Holocene temperatures (Mann et al. 1999, Briffa et al. 2001, Esper et al. 2002, Moberg et al. 2005). For oaks, climate reconstructions have generally been aimed at isolating precipitation or drought signals (Stahle and Hehr 1984, Sieg et al. 1996, St. George and Nielsen 2002, Speer et al. 2009, White et al. 2010, Stambaugh et al. 2011). However, the use of quantitative wood anatomy can in some cases reveal a signal distinct from tree-ring characteristics (Fonti et al. 2010).

To interpret the wood anatomy of subfossil oaks we investigated whether wood anatomy differed among years with cold or warm springs for extant trees from

three sites across the current range of bur oaks. The climate conditions across years and regions should span a large portion of the climatic envelope in which this species can persist. Hence, the objectives of this research were to (1) determine whether wood anatomy of extant bur oaks responds consistently to spring temperatures across sites, (2) determine methods to compare anatomical characteristics of variously degraded subfossil oaks to modern wood for temperature reconstructions, (3) compare the potential conductivity of the vasculature at each modern sample location to that of subfossil oaks, and (4) determine whether patterns in deposition of subfossil oaks into alluvial sediments, presumably near their northern range limit, were synchronous with North Atlantic climate events or displayed a time-transgressive pattern.

## METHODS

### *Study areas for modern oaks*

Tree cores from extant bur oaks were collected in 2009 from near the south-central portion of their range in Missouri (MO), the northeastern range edge in Wisconsin (WI), and the northwestern range edge in South Dakota (SD) (Fig. 1; see Plate 1). The modern climate in MO is characterized by hot summers and winters with periodic cold air masses from Canada (Table 1). Summers are often humid and wet, but severe droughts also occur depending on the degree of zonal flow and advective moisture transport from the Gulf of Mexico by low level jets (Higgins et al. 1997, Mo et al. 1997, Mo and Berbery 2004, Ting and Wang 2006). The climate in northwestern WI is much cooler than MO. In addition

to latitudinal effects, the proximity of the collection site to Lake Superior, ~5 km north, contributes to lower growing season temperatures (Table 1). Southwestern SD is much drier than the eastward range of bur oak (Table 1). Although the latitude is more similar to the WI site, SD has warmer spring and summer temperatures more similar to MO.

#### *Sample collection for modern oaks*

In each region three to four representative stands were sampled within a riparian area or just adjacent to perennial streams or rivers. From each region, increment cores from 29 to 47 trees were collected. In MO, stands were sampled from in the vicinity of the Baskett Wildlife Area. In WI stands were sampled from Brule River State Forest near Lake Superior. In SD, stands were sampled from four drainages in the eastern half of Custer State Park. Only trees that were in a dominant, codominant, or intermediate canopy position were sampled. Trees with any outward signs of past damage or symptoms of severe suppression were not sampled. From each tree an increment borer was used to extract two 5.15 mm diameter cores at breast height from perpendicular radii.

#### *Preparation and cross-dating of increment cores*

Increment cores to be measured for ring-widths were glued on wooden mounts and sanded with progressively finer sandpaper. The ring-widths were measured to 0.01-mm precision using a stereo microscope interfaced with a Velmex measurement system (Velmex, Bloomfield, New York, USA). For cross-dating, marker years were visually identified on each core and compared with known dates of wet and dry years in the region. Second, the computer program COFECHA (Holmes 1983) was used to control the dating of the series statistically (Grissino-Mayer 2001).

#### *Sample collection and radiocarbon dating for subfossil wood*

The subfossil wood resource has been described in detail elsewhere (Guyette and Stambaugh 2003, Guyette et al. 2008, Stambaugh and Guyette 2009, Stambaugh et al. 2011). Briefly, samples were collected from subfossil oak logs from streams and stream banks from northwestern Missouri (Guyette et al. 2008; see Plate 1). Stream channels and banks are composed of alluvial sediments conducive to the frequent burial and excavation of wood (Brown 1997, Guyette et al. 2008). Samples were identified by the extensive radial cracks on the exterior surface diagnostic of subfossil oak wood (Nilsson and Daniel 1990, Schniewind 1990). In addition, oxidation of phenolic compounds in the heartwood of subfossil oaks yields a gray or near-black exterior hue after 200–400 years of burial, distinguishing them from the brown hues that characterize other species. Generally, only samples with more than about 100 rings were collected. Sample locations were accessed

TABLE 1. Locations and climatic characteristics for modern bur oak (*Quercus macrocarpa*) sampling sites in Missouri, Wisconsin, and North Dakota, USA.

Climate characteristic	Missouri	South Dakota	Wisconsin
Latitude (°N)	38.8	43.7	46.7
Longitude (°W)	92.3	103.5	91.6
Temperature (°C)			
Jan mean	-1.4	-4.6	-11.4
Jul mean	25.4	21.3	18.8
Spring min	9.5	8.9	7.0
Spring mean	11.5	11.0	9.8
Spring max	14.5	13.9	11.4
February–April mean	6.5	0.7	-3.1
March–May mean	12.3	5.8	3.4
April–June mean	17.8	11.8	9.5
Annual precipitation (mm)			
Min	553	252	427
Mean	973	450	719
Max	1588	749	1028
Annual precipitation – annual ET (mm)			
Min precip – mean ET	312	102	337
Mean precip – mean ET	770	327	617
Maximum precipitation – mean ET	1499	611	960
Growing season RH (%)			
Min	74.3	61.9	71.7
Mean	81.8	70.0	79.4
Max	86.8	78.1	87.8

*Notes:* Climate data are from PRISM estimated monthly means from 1895 to 2008. Mean temperatures were calculated from the average of the mean daily maximum (max) and minimum (min) temperatures. Spring temperatures correspond to the calculation of the weighted monthly means (see *Methods*). Growing season values were calculated by averaging the monthly values weighted by the relative proportion of growing degree-days for that month. Relative humidity (RH) values were estimated from mean temperatures and dew-point temperatures. Mean annual evapotranspiration (ET) estimates were estimated from 0.5° gridded mean values from the years 2001–2006 (after Mu et al. [2007]).

by canoe and log cross sections were collected with a chainsaw.

Small blocks (~20–30 g, 10 rings) were removed from the outer edge of each log cross section for radiocarbon dating. Radiocarbon dating was conducted on acid-alkali-acid-treated wood samples by independent commercial laboratories (Geochron Laboratories, Chelmsford, Massachusetts, USA; Beta Analytic, Miami, Florida, USA), which provided radiometric measurements of <sup>14</sup>C content and radiocarbon ages. Ages are based upon the Libby half-life (5570 years) for <sup>14</sup>C and corrected for isotopic (<sup>13</sup>C/<sup>12</sup>C) fractionation. CALIB version 6.0 software (Stuiver and Reimer 1993) and the INTCAL09 calibration data set (Reimer et al. 2009) were used to calibrate the radiocarbon ages obtained with radiometric decay-count methods. A summary of drainage locations, radiocarbon laboratory codes, age estimates, and errors for each subfossil cross section is given elsewhere (see Supplement).

*Microscopy methods and sampling*

For wood anatomical measurements on modern oaks, a subset of cores from 10 or 12 trees per region were selected that did not display fire scars, insect damage, or severe growth suppression events. For wood anatomical measurements we used only cores that approached the pith so cambial ages could be estimated accurately. Cross-dated tree-rings for these years were identified on each core and shaved with a razor blade for imaging. A digital camera interfaced with the binocular microscope was used to capture images from each tree-ring. The objective lens of the microscope was set to a power of 4×, leading to a 40× total magnification.

Wood anatomy was measured for 53 of the 79 radiocarbon dated subfossil oaks. Some oaks that were particularly degraded and difficult to prepare for light microscopy were not measured. For each log cross section we used a small radial wedge of wood (1–4 cm tangential thickness at the outer, oldest edge of the wedge). Thin transverse slices of wood were taken using a razor blade from the innermost, middle, and outermost locations to provide a wide range of cambial ages for each wedge, and the average cambial age of the tree-rings was recorded. These hand-sections were observed through a Nikon Eclipse E400 light microscope (Nikon, Melville, New York, USA) using a 10× objective lens, leading to a total magnification of 100×. Multiple digital images, arranged tangentially, were obtained from the same wood wedge for each cambial age. Some subfossil oak wood cross sections that were too degraded to make thin hand-sections were frozen in liquid nitrogen, cracked along the transverse plane, and imaged as described previously for the modern wood.

*Linking climate data and the timing of earlywood vessel growth in spring*

Temperatures at each site for the years 1895–2008 were estimated from monthly interpolated meteorological data obtained from the PRISM Group at Oregon State University (*available online*).<sup>6</sup> For each region, six calendar years were identified with the purpose of spanning the widest range in spring temperature values possible at each site. All else equal, preference was given to more recent calendar years (post-1950) because the raw meteorological data that PRISM interpolations are based upon were more widely and consistently collected during this period. Cambial activity and earlywood (EW) formation of oaks starts before budburst (Ahlgren 1956, Dougherty et al. 1979, Atkinson and Denne 1988). About 2–6 weeks before budbreak, overwintering cells in the cambial region start expanding before the initiation of cell division (Zasada and Zahner 1969, Frankenstein et al. 2005). EW vessels tend to mature after 4–5 weeks (Zasada and Zahner 1969, García-González and Eckstein 2003). Hence with 1–3 rows of

EW vessels per ring being most common, it would take 4–15 weeks to complete EW formation in most years.

Bur oak budburst occurs 1–2 weeks before flowering and tends to coincide with the month when the mean temperature is near 10°C (Leopold and Jones 1947, Ahlgren 1957, Bell and Johnson 1975, Wang et al. 1992; R. Guyette and S. Voelker, *personal observation*). Interannual variation in the phenology of bur oaks can change by about a month depending on the temperature regime for that year (Ahlgren 1957). To capture variation in the phenology of EW formation better than a simple mean, we calculated a weighted mean temperature for the three months that corresponded to EW formation at each site. These were the months of March–May for MO and April–June for WI and SD. The calculation puts greater weights on the temperatures for those months that are closest to 10°C and standardizes the weights with respect to the sum of the deviations from 10°C such that the sum of the weights is always equal to one. For example, mean monthly temperatures for March–May in MO for 1905 were 9.74°, 12.39°, and 18.11°C. These resulted in weights of 0.49, 0.39, and 0.12 and would correspond to favorable temperatures for EW formation during a relatively warm March and only a small influence of the May temperatures by which time EW formation would largely have been completed. By contrast, in 1906 the temperatures were 0.07°, 14.60°, and 18.69°C. The weights for these months were 0.28, 0.40, and 0.31 and correspond to less EW cambial activity during a cold March and a greater influence of April and May.

Monthly precipitation data were obtained from the PRISM website. Similarly, relative humidity values were estimated with monthly average temperature and dew-point data from the PRISM website. To test for the effects of drought on tree-ring variables and anatomy we obtained monthly Palmer drought severity index (PDSI) values for the nearest climate division for each sample region from 1895 to 2008 from the IRI/LDEO climate data library (*available online*).<sup>7</sup> We used data from Climate Division Two in MO, Division One in WI, and Division Four in SD. Annually averaged evapotranspiration (ET) estimates were estimated from eight-day means of meteorological data and MODIS remotely sensed data for the years 2000–2006 (Mu et al. 2007, 2009) at the scale of 0.05° and then scaled up to a 0.5° regional average.

*Quantitative wood anatomical measurements*

We measured EW anatomical characteristics and EW and latewood widths with ImageJ software (National Institutes of Health, Bethesda, Maryland, USA; *available online*)<sup>8</sup>. We calculated mean EW vessel diameters from the individual vessel areas as  $d = 2 \times \text{SQRT}(a/\pi)$  where  $d$  is vessel diameter,  $a$  is the area of each vessel, and SQRT is square root. In many cases, subfossil oak

<sup>6</sup> <http://www.prism.oregonstate.edu/>

<sup>7</sup> <http://iridl.ldeo.columbia.edu/>

<sup>8</sup> <http://rsb.info.nih.gov/ij/>

vessels were collapsed to some degree in the radial plane such that the tangential diameters of their vessels were lesser than would be expected. To obtain measurements that were comparable to modern values from subfossil trees that were variously degraded or distorted during the preparation of slides (Appendix: Fig. A1), we instituted a correction to each vessel diameter. The collapse corrected diameter was calculated as:  $(1/\pi) \times (\text{SQRT}(\text{vessel area measured} \times 0.93/a\%))$ , with  $a\%$  = vessel area measured/vessel area calculated from the perimeter/ $\pi$ , assuming circularity, and 0.93 is the average value for EW vessels from normal, non-collapsed wood. The calculation of  $a\%$  assumed the perimeter was equal to the circumference of a circle (i.e.,  $d = \text{perimeter}/\pi$ ). Hence,  $a\%$  represents the degree to which a vessel is elliptical or collapsed due to diagenesis and sample preparation (i.e., an  $a\%$  equal to one would be a perfect circle).

For each image we measured the ring-width, early-wood to latewood ratio (EW/LW), EW vessel frequency (EWF, number of EW vessels divided by the wood area imaged) and EW lumen area (EWA, the sum of EW vessel areas divided by the total wood area imaged). The imaged wood areas used for the calculation of EWF and EWA were corrected to reflect the difference induced by vessel collapse. We also calculated the EW specific vessel frequency and lumen area (EWF<sub>s</sub> and EWA<sub>s</sub>, respectively) by dividing EWF and EWA by the EW proportion (i.e., EW/EW + LW) of each image.

From the collapse-corrected EW vessel diameters (EWD) we calculated the EW hydraulic diameter (EWD<sub>h</sub>), the area-weighted EW vessel diameter (EWD<sub>a</sub>), and the EW specific theoretical conductivity (EWK<sub>s</sub>). EWD<sub>h</sub> was calculated as the average of  $\Sigma d^5 / \Sigma d^4$ , where  $d$  is the diameter of each vessel in a sample. EWD<sub>h</sub> weights individual conduit diameters to correspond to the average Hagen-Poiseuille lumen theoretical hydraulic conductivity for that vessel size (Sperry and Ikeda 1997). Area-weighted diameter, EWD<sub>a</sub>, was calculated as the average of each vessel diameter squared ( $\text{EWD}_a = \text{SQRT}(\Sigma d^2)/n$ ). EWD<sub>a</sub> was used to plot against vessel frequency so that each axis was scaled according to differences in vessel area. EWK<sub>s</sub> was estimated as  $(\rho \times \pi \times \Sigma r^4)/(128 \times \mu \times A)$ , where  $\rho$  is the density of water at 20°C,  $r$  is the radius,  $\mu$  is the viscosity of water, and  $A$  is the area imaged after being adjusted for EW proportion.

Another variable of potential interest is the most commonly occurring vessel size, or the modal EWD. For modern wood modal EWD was calculated by fitting each individual vessel measurement into 20- $\mu\text{m}$  bins and identifying the most commonly occurring bin size for each temperature and site combination. For subfossil wood the same procedure was calculated for each sample and cambial age combination.

Many aspects of wood anatomy display radial variation in the stem, from pith to bark (Lachenbruch et al. 2011). It is therefore necessary to standardize for

cambial age for accurate comparisons of wood anatomical measurements among groups that may differ in their age distributions. Conceptually this process is similar and has some of the same benefits and drawbacks as the regional chronology standardization method developed for dendrochronology (Briffa and Melvin 2008). For comparisons of EWD, modal EWD, or EWD<sub>h</sub> each individual EW vessel diameter  $d$  was standardized to age 50 following region-specific cambial age trends (Fig. 2). The percentage deviations from the regression predicted value for a given cambial age were calculated for each vessel measurement. These percentage deviations were then multiplied by the vessel size values predicted for age 50 (an age common to all subsets of the data) by the cambial age regression for that subset of the data. For comparisons of EWK<sub>s</sub> among groups the same age standardization procedures were applied to values for each cambial age rather than for individual vessel measurements.

#### *Proxy development from wood anatomical data*

It was initially sought to develop linear transfer functions based on the relationship between EW anatomical characteristics and spring temperatures. In contrast to anatomical data from modern wood that were based on measurements from a number of trees from a known year, measurements from subfossil wood were necessarily based on one or a few rings within a single tree and thus will often fall outside of the range covered by a proxy relationship. Values outside of the predicted range are problematic because the relationship between vessel size and temperature must be sigmoidal across a large temperature span. An overview of modifications to linear relationships is provided elsewhere (see Appendix: Tables A1 and A2).

#### *Comparisons to other proxy data*

To investigate changes in oak anatomy through time and the frequency of subfossil wood deposition in alluvial sediments, we compared our data to three other proxy records. The first two are thought to be indicative of changes to temperatures and/or atmospheric circulation relevant for the conditions that may have been encountered over the American mid-continent during the late Quaternary. These included NGRIP ice core  $\delta^{18}\text{O}$  (NGRIP members 2004), a proxy for changes in temperature over the circum-North Atlantic region, Cariaco grayscale, a marine sediment record thought to record variation in upwelling caused by differences in the strength of trade wind flow from the Atlantic into the Caribbean sea (Hughen et al. 1996, 2000), and July temperatures over the Midwest (Viau et al. 2006) that were modeled from a network of spatially explicit pollen or sediment core data (Grimm 2000).

#### *Statistical analyses*

To examine the effects of temperature and origin (i.e., region or time period) and their interaction on wood

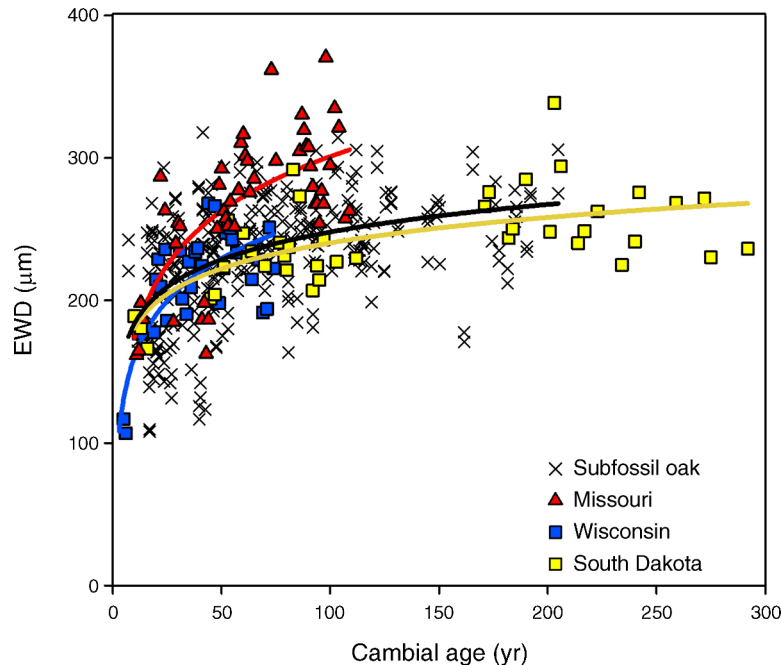


FIG. 2. Earlywood vessel diameter (EWD) plotted against cambial age for oaks from the three modern sampling areas and for the subfossil wood collected from northern Missouri.

anatomy, two-way analysis of variance tests were conducted with PROC Mixed, SAS software version 9.2 (SAS Institute, Cary, North Carolina, USA). PROC Mixed was run using the restricted maximum likelihood estimation method. In comparing subfossil to modern wood, origin could refer to the three sample locations for modern oaks or for the three relevant time periods for the subfossil oaks (i.e., Bølling-Allerød [B/A], YD, and the Pre-Boreal [PB] transition from the YD to the early Holocene). We also used standard major axis tests and routines (SMATR) program version 2.0 (Warton et al. 2006) to compare whether EWF or EWF<sub>s</sub> scaled with EWD<sub>a</sub> similarly among modern and subfossil wood origins. Where slopes of the scaling relationships were not different, the same software was employed to conduct post hoc WALD tests for shifts in elevation or for shifts along the common slope.

## RESULTS

### *Wood anatomical characteristics differ among wood origins*

EWD increased with cambial age at each of the collection sites for modern wood (Fig. 2). The age-related trajectory of EWD was steepest for MO oaks, reaching an average EWD of ~250 µm at age 50. By contrast, EWD at age 50 for WI, SD, and subfossil oaks were all ~220 µm. As expected from global patterns in wood anatomy, EWF had a negative relationship with EWD<sub>a</sub> for both modern and subfossil wood (Fig. 3a). The scaling relationships with EWD<sub>a</sub> depended on whether the number of EW vessels were considered per

unit wood area (EWF; Fig. 3a) or per unit EW area (EWF<sub>s</sub>; Fig. 3b). EWD<sub>a</sub> predicted EWF<sub>s</sub> better for both modern and subfossil oaks ( $r^2 = 0.48$  and  $0.64$ , respectively) than for EWF ( $r^2 = 0.26$  and  $0.58$ , respectively). Linear regression lines fit to log-transformed EWF<sub>s</sub> vs. EWD<sub>a</sub> showed no significant difference ( $P = 0.77$ ) between the slopes of the scaling relationships for modern vs. subfossil oaks (Fig. 3b, inset).

For a given EWD<sub>a</sub>, EWF<sub>s</sub> was ~40% greater (i.e., more hydraulically efficient) for subfossil oaks than modern oaks ( $P < 0.0001$ ) (Fig. 3b; Appendix: Table A3). Subfossil oaks also had greater EWF<sub>s</sub> for a given EWD<sub>a</sub> when compared against the relationships for MO, SD, and WI (Appendix: Table A3). Among the modern sites MO oaks had greater EWF<sub>s</sub> values for a given EWD<sub>a</sub> than SD or WI (Appendix: Table A3). The scaling of vessel frequency with vessel size was surprisingly similar among three late Quaternary time periods (B/A, YD, and PB); the PB had significantly lower EWF<sub>s</sub> for a given EWD<sub>a</sub> than the B/A, but the other pairwise comparisons were nonsignificant (Appendix: Table A3). Subfossil oak vessel characteristics were shifted upward (more hydraulically efficient) compared to the modern oaks as a whole. However, subfossil oak vessels were also shifted to the left, (less hydraulically efficient) compared to trees from MO and WI, and were not different than those from SD (Fig. 3b; Appendix: Table A3). Compared to oaks from SD and WI, MO oaks were shifted significantly lower and to the right along the common slope, toward the most hydraulically

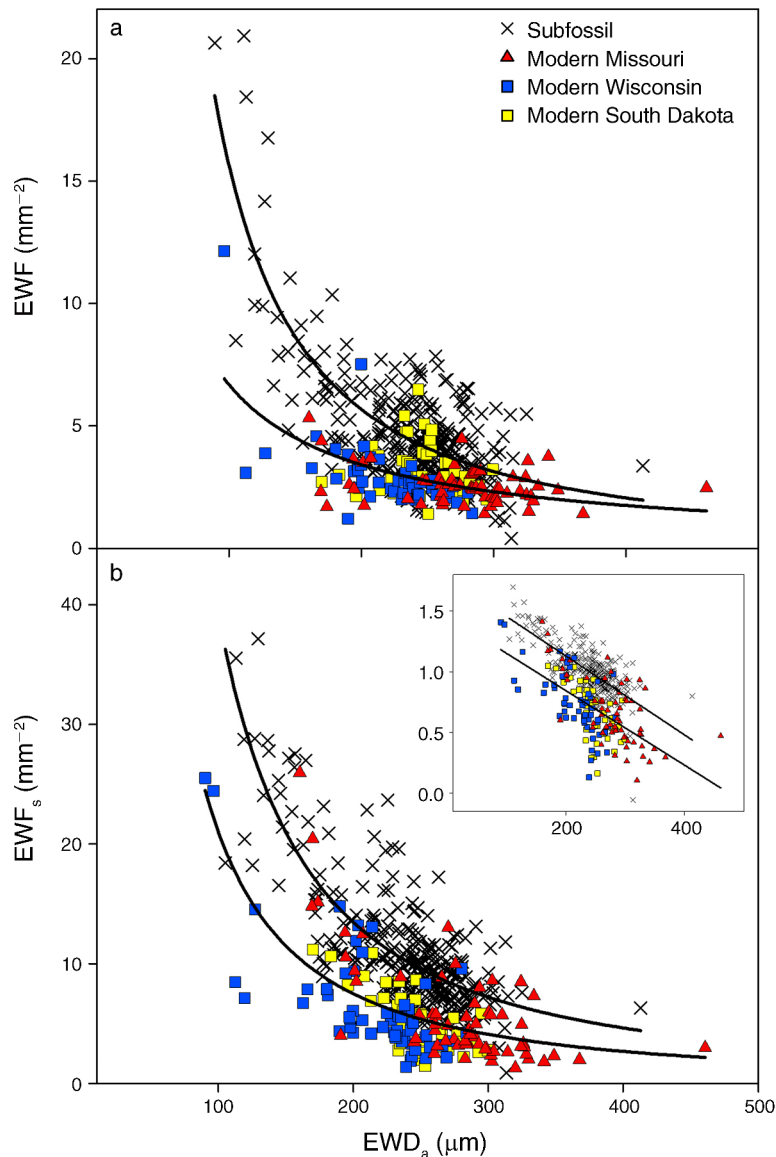


FIG. 3. Earlywood vessel frequency (EWF) and earlywood specific vessel frequency ( $EWk_s$ ) plotted against area-weighted earlywood vessel diameter ( $EWD_a$ ) for modern and subfossil oak wood. The inset in the lower panel is the logarithm of  $EWk_s$  plotted vs.  $EWD_a$ . Subfossil oak data are corrected for collapse.

efficient position, while SD oaks were shifted lower and to the right from WI oaks, making oaks from the cold WI site the least hydraulically efficient (Fig. 3b; Appendix: Table A3). There were no shifts along the common slope among the modern vs. subfossil oaks from the B/A, YD, and PB.

The functional significance for xylem hydraulic efficiency imparted by shifts in EWF for a given EWD or shifts along a common scaling slope can be summarized in a single value, the EW specific theoretical conductivity,  $EWk_s$ . For each group  $EWk_s$  increased with cambial age (Fig. 4), paralleling the age-related patterns in EWD (Fig. 2). There was more scatter in  $EWk_s$  than in EWD, and the trajectory rankings were

consistent with the age-related trends in EWD (Figs. 2 and 4). For modern MO oaks the slope of  $EWk_s$  vs. log-transformed cambial age was significantly greater ( $P \leq 0.043$ ) than the slopes for oaks from WI and SD as well as the B/A, YD, or PB. In contrast, the slopes for WI and SD trees were lower ( $P \leq 0.066$ ) than subfossil oaks from each of the three late Quaternary periods. There were no significant differences in slopes among oaks from the B/A, YD, or PB ( $P \geq 0.692$ ).

*Modern wood anatomical characteristics are affected by spring temperatures*

We sought to determine whether spring temperatures and/or drought affected oak wood anatomy consis-

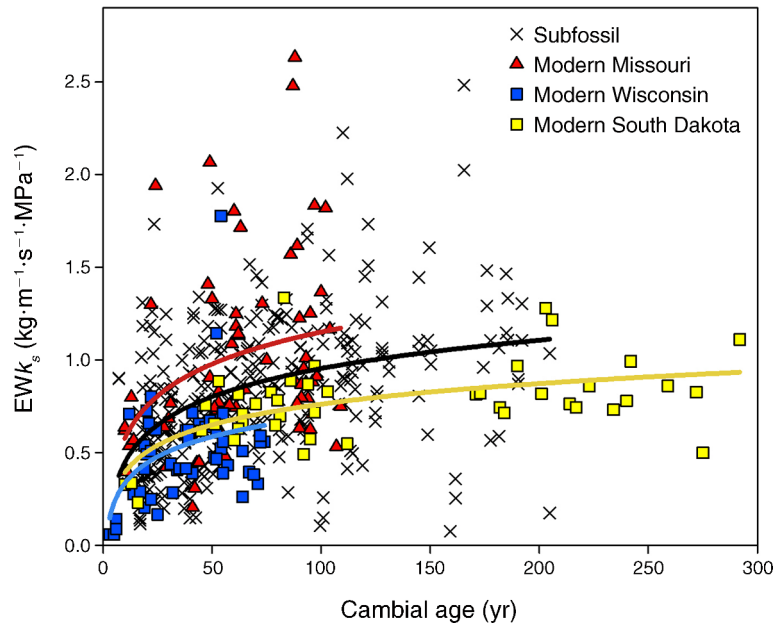


FIG. 4. Earlywood specific conductivity ( $EWk_s$ ) plotted against cambial age for the three modern wood collection sites and the subfossil oaks.

tently among years and across regions. Both  $EWD$  and  $EWD_h$  of modern oaks were correlated significantly with spring temperatures across years and sites ( $P = 0.0013$  and  $P = 0.0155$ , respectively; Fig. 5a). Although the regression of  $EWD$  vs. temperature was significant, ANOVA results indicated that temperature effects on  $EWD$  were not significant ( $P = 0.08$ ) after accounting for the effects of origin (Table 2). ANOVA results provided additional evidence that temperature had a significant ( $P = 0.04$ ) effect on  $EWD_h$  (Table 2). Modal  $EWD$ ,  $EW$  specific lumen area,  $EWA_s$ , and  $EWk_s$  were significantly correlated with temperature ( $P < 0.0001$ ,  $P < 0.0001$ , and  $P = 0.0105$ , respectively; Fig. 5b–d). According to the ANOVA results, temperature significantly affected each of these anatomical characteristics ( $P < 0.01$ ,  $P = 0.02$ , and  $P = 0.02$ , respectively; Table 2). The lack of significant origin  $\times$  temperature interactions indicated temperature responses were similar across regions (Table 2). Warmer temperatures increased the frequency of larger diameter vessels and decreased the frequency of smaller vessels (Fig. 6). Standardizing  $EWk_s$  to cambial age 50 (see *Methods*) revealed that the mean value ( $\text{kg}\cdot\text{m}^{-1}\cdot\text{s}^{-1}\cdot\text{MPa}^{-1}$ ) for MO (1.11) was significantly larger ( $P \leq 0.0002$ ) than the means for SD (0.68) and WI (0.64) (Fig. 4). Using the same regression and ANOVA analyses we found no significant relationships ( $P > 0.05$ ) between  $EWD$ , modal  $EWD$ ,  $EWD_h$ ,  $EWA_s$ , and  $EWk_s$  and Palmer drought severity index (PDSI) values for the spring months of the year sampled or of the previous growing season (data not shown).

#### *Comparisons of subfossil oaks and other paleoclimate proxies*

With respect to modern spring temperatures in MO, temperatures estimated from subfossil wood averaged  $\sim 3^\circ\text{C}$  lower, corresponding more closely to the modern temperature regime at the cold northeast edge (WI) of the species range (Fig. 7a). The warmest periods of the deglaciation occurred near the ends of the B/A and PB periods (Fig. 7a). The coldest spring period in MO was at the beginning of the oak record at 13.6 ka (Fig. 7a). The warming trend in spring temperatures from the YD through the PB is broadly synchronous with the trends in the NGRIP  $\delta^{18}\text{O}$  record (Fig. 7a). Similar to trends in spring temperatures, subfossil oak hydraulic efficiency, as indicated by  $EWk_s$ , had a slowly increasing trend from the YD through the end of the PB (Fig. 7a, b). The warm spring temperatures at the end of the B/A period were associated with  $EWk_s$  of subfossil oaks nearly matching the values of modern MO oaks. Low  $EWk_s$  values of subfossil oaks corresponded to cold spring temperature estimates at the beginning of the oak record near 13.6 ka as well as on either end of the YD.

A sharp reduction in the 200-year running frequency of bur oak deposition was coeval with the beginning of the YD where there were reductions in NGRIP  $\delta^{18}\text{O}$ , Cariaco grayscale, and July Midwest temperatures (Fig. 7a–c). A 400-year hiatus in oak deposition (12.25–12.66 ka), the longest within this record, followed the decline in spring temperatures and  $EWk_s$  after the onset of the YD (Fig. 7). Given our sampling intensity of subfossil oaks from 9.9 to 13.63 ka, the probability of sampling only 14 oaks dated within the 1300 year long YD is very

low ( $P < 0.003$ ). Besides the low depositional frequency during the YD, the 200-year running frequency of  $^{14}\text{C}$ -dated oaks is dominated by a peak near 11.0 ka. This peak in depositional frequency is notably large considering that on average only five to six subfossil logs were sampled thus far during each 200-year period from 13.62 to 0.40 ka (R. Guyette, *unpublished data*). Although this pulse of oak deposition does not match well with NGRIP  $\delta^{18}\text{O}$  and Cariaco grayscale, there still existed significant correlations between the 200-year running frequency of  $^{14}\text{C}$ -dated oaks and NGRIP ice core  $\delta^{18}\text{O}$  ( $r = 0.44$ ,  $P < 0.001$ ) as well as with Cariaco grayscale ( $r = 0.36$ ,  $P < 0.001$ ), indicating substantial agreement between North Atlantic temperatures, trade wind strength entering the Caribbean from the Atlantic, and oak deposition in northwestern MO. There was also a strong correlation ( $r = 0.42$ ,  $P < 0.001$ ) between the pulse of oak deposition and July temperatures inferred for the Midwest from transfer functions applied to pollen data (Fig. 7c). In comparison to all three of the independent proxies, correlations were higher if the dating of oak deposition was shifted earlier in time by 100–250 years.

#### DISCUSSION

Spring is a critical period for oaks because EW formation, flowering, wind-driven pollen dissemination, shoot extension, and leaf expansion all must occur in a certain order, sometimes simultaneously, and only during a relatively short period. Compared to summer conditions, relatively small differences in spring temperatures or water deficits may thus have disproportionately large effects on tree and ecosystem function. Temperate oak species will have some capacity for interannual shifts in phenology, resulting in spring temperature signals in tree-rings being attenuated compared to the actual temperatures in a given month. However the ability to resolve centennial to millennial scale variation in spring climate from this wood anatomical proxy is a valuable new tool for paleoclimate reconstruction. Greater accuracy and resolution should be possible if more samples are collected and if more intensive, interannual analyses are undertaken.

*Earlywood characteristics provide consistent proxies for spring temperature across the bur oak range*

We sampled oak wood across time and space to cover a large portion of the climate space in which bur oak occurs (Fig. 1, Table 1). Although bur oak can grow much farther to the south than we sampled, inventory data from the USDA Forest Service indicate that the core area of this species is largely from MO northward (Fig. 1; Burns and Honkala 1990). Across climatically different regions, spring temperatures had a consistent effect on EW vessel dimensions (Fig. 6). As in most dendrochronological studies, the strength or even direction of the climatic signal obtained from EW vessel

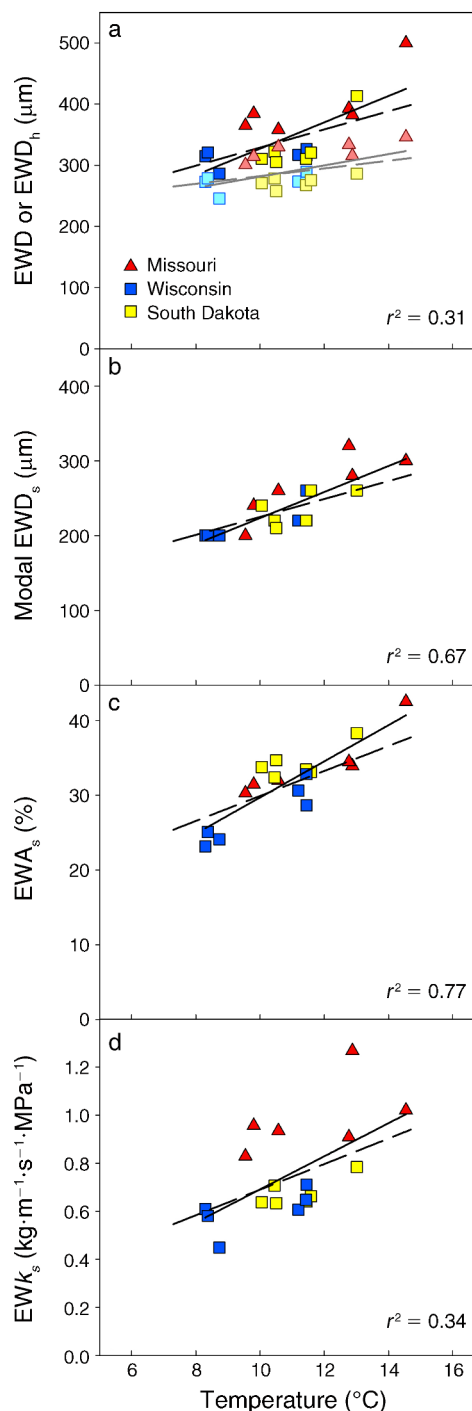


FIG. 5. (a) Earlywood vessel diameter (EWD, light symbols) and earlywood vessel hydraulic diameter ( $\text{EWD}_h$ , dark symbols), (b) modal EWD, earlywood specific lumen area ( $\text{EWA}_s$ ), (c)  $\text{EWA}_s$  as a percentage, and (d) earlywood specific conductivity ( $\text{EWk}_s$ ) plotted against spring temperatures. Anatomical measurements were corrected to a common cambial age of 50 years. The coefficients of determination refer to the solid line as fit to the points shown. The dashed lines represent the regression line of each wood anatomical variable as fit to mean temperatures of April–June in Missouri and May–July for Wisconsin and South Dakota.

TABLE 2. ANOVA results for selected anatomical characteristics of modern oak wood comparing the effect of temperature, origin, and their interaction.

Anatomical variable and source	df	F	P
<b>EWD</b>			
Origin	2, 15	0.20	0.82
Temp	1, 17	3.61	0.08
Temp $\times$ origin	2, 15	0.09	0.92
<b>EWD<sub>h</sub></b>			
Origin	2, 15	1.37	0.29
Temp	1, 17	4.83	0.05
Temp $\times$ origin	2, 15	0.61	0.56
<b>Modal EWD</b>			
Origin	2, 15	0.21	0.81
Temp	1, 17	14.68	<0.01
Temp $\times$ origin	2, 15	0.48	0.63
<b>EWA<sub>s</sub></b>			
Origin	2, 15	0.04	0.96
Temp	1, 17	7.67	0.02
Temp $\times$ origin	2, 15	0.05	0.95
<b>EWk<sub>s</sub></b>			
Origin	2, 15	0.04	0.97
Temp	1, 17	6.63	0.02
Temp $\times$ origin	2, 15	0.34	0.72

Note: Data for earlywood diameter (EWD), earlywood hydraulic diameter (EWD<sub>h</sub>), modal EWD, earlywood specific lumen area (EWA<sub>s</sub>), and earlywood specific theoretical k<sub>s</sub> (EWk<sub>s</sub>) were corrected for age before analyses.

dimensions also depends crucially on the species selected and the local growing conditions. In oaks growing in a dry valley of the Swiss Alps, EW vessel area had a significant negative relationship with a drought index of the previous fall and current summer conditions (Eilmann et al. 2006). Under these conditions the strength of the drought signal apparently overwhelmed a spring temperature response. By contrast, oaks growing on mesic sites had a significant negative relationship with spring precipitation and a positive relationship with spring temperatures (Fonti and García-González 2008). The ring-porous species chestnut (*Castanea sativa* Mill.) also had a positive response of EW vessel area to spring temperatures (Fonti et al. 2007).

Oaks growing in a maritime environment had significant, positive correlation between EW vessel area and spring precipitation and negative correlations with spring temperatures (García-González and Eckstein 2003). This study of oaks differs from the rest in the sign of the temperature response of EW vessel size. A difference in the sign of the response may stem from measuring a temperature response at a site that is above the optimum temperature for this species rather than from the center of the range toward the north as in the oaks we studied. Indeed, the oaks studied by García-González and Eckstein (2003) were near their south-westerly range limit in Spain. From a functional perspective, cold spring temperatures will often limit

EW vessel size and thus reduce wood hydraulic efficiency. In some cases this could cause an unexpectedly high sensitivity of growth to summer drought stress after springs with low temperatures. Likewise, because warm springs may reduce EW vessel size in oaks near their southern range limit (García-González and Eckstein 2003), periodic droughts may be even more acutely sensed after a warm spring. Because warm spring temperatures would tend to increase growing season length, transpiration, and the depletion of stored soil water, this spring temperature and summer drought stress interaction should be more pronounced at range limits generally delimited by drought stress. This may help explain why mature bur oaks in Texas regularly display extensive shoot dieback (M. Stambaugh, *personal observation*), a condition that is relatively rare across the northern extent of the range.

Many physiological responses to temperature have been studied extensively in experiments and field studies of woody species. However results are usually expressed with respect to a change in average growing season temperature, and measurements of wood anatomical responses are few (Way and Oren 2010). Within a certain range of phenotypic and photoperiodic constraints, cold spring temperatures will generally shift growth and phenology later in the season. However, our results demonstrate that there is still an effect of temperature on EW dimensions even if the mean spring temperatures were used for analyses rather than weighted spring temperatures that helped account for shifts in EW formation dates (Fig. 5). Most studies of the low-temperature controls on growth in woody species have focused on conifers. Compared to ring-porous oaks, conifers differ in form, function, and habitat preferences. These differences may influence

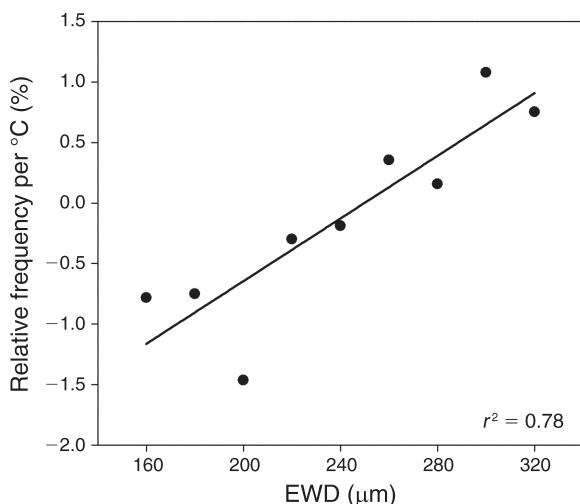


FIG. 6. The change in the relative frequency of earlywood vessel diameters (EWD) per unit temperature (i.e., %/°C) plotted vs. EWD in 20- $\mu$ m bins. The data are from all three sites together. Only bins with  $\geq 5\%$  of the total number of vessels measured are shown.

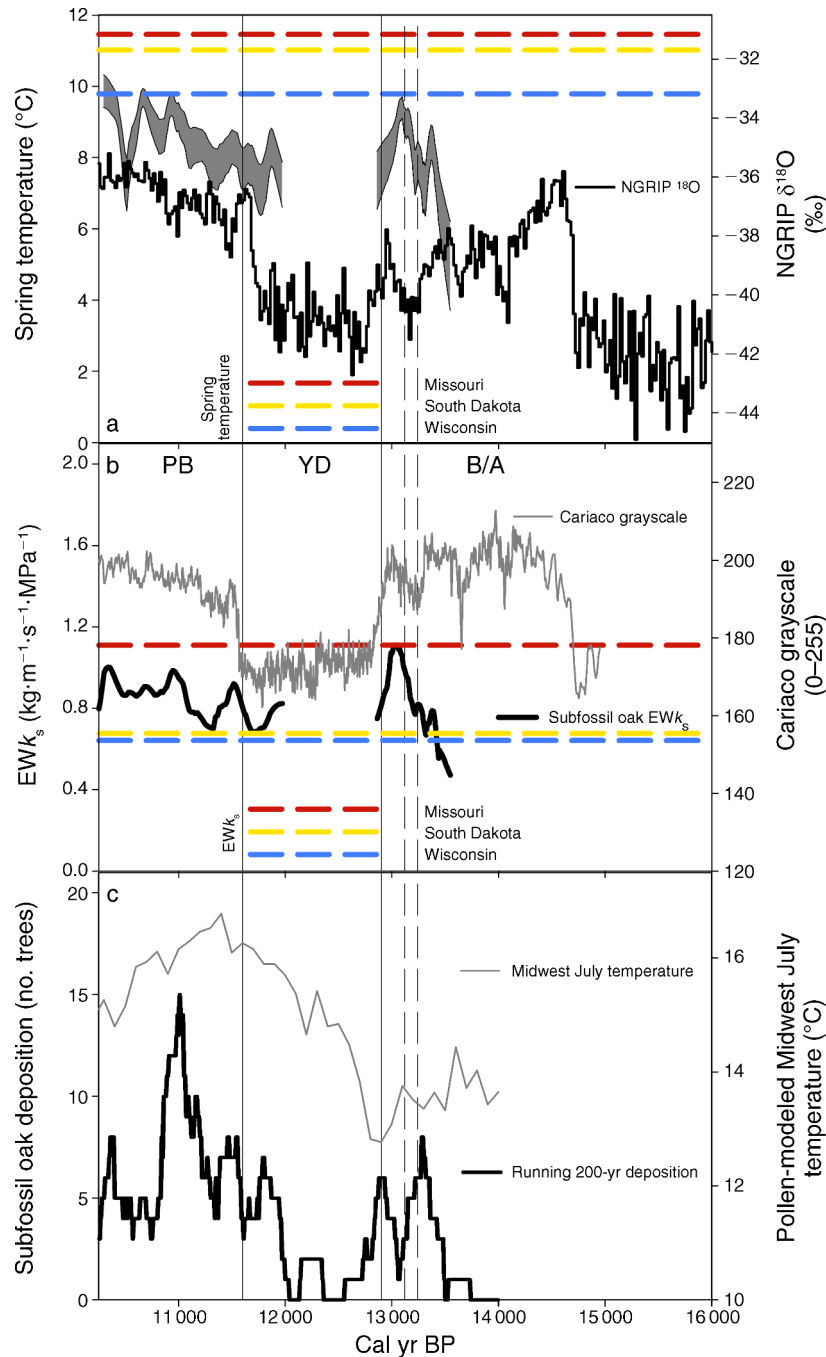


FIG. 7. Late Quaternary trends in spring temperature estimates, earlywood specific conductivity ( $EWk_s$ ), and oak recruitment frequency are compared to Greenland ice core (NGRIP members 2004)  $\delta^{18}O$ , Cariaco grayscale (Hughen et al. 2000), and Midwest July temperatures modeled from the pollen record (Viau et al. 2006). The solid vertical lines demarcate the Younger Dryas (YD) cold event from the Bølling-Allerød (B/A) and the Pre-Boreal (PB) periods. Dashed vertical lines demarcate the beginning and end of the inter-Allerød cold period. Temperature estimates for MO are from the mean response of four proxies; mean EW vessel diameter (EWD), modal EW vessel diameter (modal EWD), EW hydraulic diameter ( $EWD_h$ ), and EW specific lumen area ( $EWA_s$ ) of subfossil oak wood (Fig. 5a-c). The gray area covers the span of the spring temperature data assuming a  $17^\circ C$  maximum spring temperature and either a  $2^\circ C$  or a  $6^\circ C$  minimum temperature required for each of EWD, modal EWD,  $EWD_h$ , and  $EWA_s$ . Modern spring temperature estimates for each site were calculated across the years 1895–2008. The temperature and  $EWk_s$  estimates from subfossil wood were plotted after undergoing a loess smoothing procedure to emphasize low-frequency trends. For each of the smoothed data sets the calibrated  $^{14}C$ -dates were adjusted in time with respect to the cambial age analyzed since only the outer rings of each log cross section were  $^{14}C$ -dated. Cariaco grayscale measures the reflectivity of an annually resolved sediment record from the Cariaco basin that is indicative of intensity of Ekman upwelling along the north coast of Venezuela ( $10^\circ 40' N$ ,  $65^\circ W$ ).

TABLE 3. Wood anatomical characteristics by sample origin (mean  $\pm$  SD).

Wood characteristic	Extant			Subfossil		
	Missouri	South Dakota	Wisconsin	Pre-Boreal	Younger Dryas	Bølling-Allerød
No. trees sampled	12	10	10	24	16	13
EWD ( $\mu\text{m}$ )	262.7 $\pm$ 47.9	225.4 $\pm$ 37.1	208.4 $\pm$ 27.8	235.4 $\pm$ 28.3	227.3 $\pm$ 45.5	225.4 $\pm$ 35.1
Age-corrected EWD ( $\mu\text{m}$ )	260.6 $\pm$ 32.1	219.6 $\pm$ 14.9	225.5 $\pm$ 23.0	233.2 $\pm$ 24.3	219.8 $\pm$ 36.6	220.4 $\pm$ 35.2
EWD <sub>h</sub> ( $\mu\text{m}$ )	320.9 $\pm$ 53.6	260.3 $\pm$ 43.6	258.2 $\pm$ 27.4	282.6 $\pm$ 32.7	274.2 $\pm$ 56.7	270.0 $\pm$ 36.5
Age-corrected EWD <sub>h</sub> ( $\mu\text{m}$ )	305.1 $\pm$ 35.3	250.8 $\pm$ 22.0	256.0 $\pm$ 27.8	280.6 $\pm$ 31.0	267.5 $\pm$ 58.6	265.6 $\pm$ 37.5
EWD <sub>a</sub> ( $\mu\text{m}$ )	271.8 $\pm$ 48.4	230.1 $\pm$ 36.1	214.2 $\pm$ 28.8	244.6 $\pm$ 29.2	235.7 $\pm$ 47.3	233.3 $\pm$ 35.2
EWf ( $\text{mm}^{-2}$ )	2.5 $\pm$ 0.74	3.2 $\pm$ 1.1	3.0 $\pm$ 1.6	3.6 $\pm$ 1.6	4.2 $\pm$ 2.3	4.1 $\pm$ 1.1
EWf <sub>s</sub> (no. early-wood vessels/mm)	6.4 $\pm$ 4.3	6.5 $\pm$ 2.9	6.8 $\pm$ 2.3	8.4 $\pm$ 3.3	9.5 $\pm$ 5.7	9.9 $\pm$ 2.4
EWA (%)	13.4 $\pm$ 1.2	13.8 $\pm$ 3.1	12.5 $\pm$ 3.6	16.3 $\pm$ 3.8	17.0 $\pm$ 3.3	16.6 $\pm$ 4.6
EWA <sub>s</sub> (%)	34.4 $\pm$ 8.8	31.9 $\pm$ 5.5	27.3 $\pm$ 4.4	37.6 $\pm$ 6.4	36.9 $\pm$ 4.7	39.2 $\pm$ 6.4
Ring-width (mm)	2.44 $\pm$ 0.98	1.62 $\pm$ 0.49	2.20 $\pm$ 0.63	1.44 $\pm$ 0.50	1.19 $\pm$ 0.32	1.23 $\pm$ 0.40
Age-corrected ring-width (mm)	2.43 $\pm$ 0.90	1.76 $\pm$ 0.38	2.01 $\pm$ 0.68	1.43 $\pm$ 0.49	1.20 $\pm$ 0.29	1.32 $\pm$ 0.37
EW/LW ratio	0.71 $\pm$ 0.38	1.08 $\pm$ 0.87	0.81 $\pm$ 0.17	0.89 $\pm$ 0.25	1.02 $\pm$ 0.43	0.86 $\pm$ 0.23
Age-corrected EW/LW ratio	0.68 $\pm$ 0.31	0.91 $\pm$ 0.61	0.92 $\pm$ 0.14	0.83 $\pm$ 0.31	0.89 $\pm$ 0.49	0.75 $\pm$ 0.33

Notes: Age-corrected values were standardized to cambial age 50. Abbreviations are: EWD, earlywood vessel diameter; EWD<sub>h</sub>, earlywood vessel hydraulic diameter; EWD<sub>a</sub>, area-weighted earlywood vessel diameter; EWf, earlywood vessel frequency; EWf<sub>s</sub>, earlywood specific vessel frequency; EWA, earlywood vessel area; and EWA<sub>s</sub>, earlywood specific vessel area.

their responses to temperature. Nonetheless some of the most basic physiological responses to temperature such as enzyme function are likely shared across these divergent lineages (Way and Oren 2010). Growth at low temperature (i.e.,  $<10^\circ\text{C}$ ) has been thought to be governed by reduced carbon demand (Körner and Hoch 2006, Hoch and Körner 2009) or a gradient between limitations by either carbon demand and supply (Bansal and Germino 2008, Susiloto et al. 2010, Sveinbjörnsson et al. 2010). Indeed, experimental stem chilling of conifer stems to below  $10^\circ\text{C}$  has demonstrated that low temperatures have a strong inhibitory effect on total carbon supply, likely via phloem transport (Johnsen et al. 2007).

In oaks, stem cambial activity starts just before or during budbreak (Zasada and Zahner 1969, Ahlgren 1957, Dougherty et al. 1979). An important factor in the initiation of xylem formation may be polar auxin transport, which was initiated at temperatures of  $0\text{--}5^\circ\text{C}$  in a temperate diffuse-porous species (Schrader et al. 2003). From ring-porous species it is known that dissolved sugars are transported to the cambium from the xylem water in the spring, but it is not fully appreciated how temperature can modulate this activity (Alves et al. 2007, Bonhomme et al. 2009). Higher stem respiration in the spring is indicative of increased growth rates, and oak stem respiration rates show a logarithmic response to spring air temperatures before leaf expansion (Edwards and Hanson 1996). However, the linear increase in vessel size (and thus cell wall material produced) across a similar temperature range (Figs. 5 and 6) indicates that vessel size is not linearly related to respiration rate.

#### *Does [CO<sub>2</sub>] affect the scaling of vessel frequency and diameter?*

Modern oaks had greater EW vessel lumen area per wood area during warmer springs (Fig. 3a, b). In comparison to modern oaks, subfossil oaks had smaller, more tightly packed EW vessels for a given EWD<sub>a</sub> (Fig. 3b) and thus had greater EWA or EWA<sub>s</sub> than modern wood (Table 3). To use EWA<sub>s</sub> as a proxy for temperature we had to institute a correction to EWf<sub>s</sub> of subfossil wood for accurate comparisons with modern wood (see Appendix). Hence, the effect of temperature on EWA<sub>s</sub> was predicated on reducing subfossil oak EWf<sub>s</sub> by  $\sim 40\%$  to match modern EWf<sub>s</sub>. It may not be a coincidence that this level of reduction corresponds well to the change in the average atmospheric [CO<sub>2</sub>] between the modern vs. subfossil oaks (ambient [CO<sub>2</sub>] was  $\sim 220$  ppm during the B/A and  $\sim 350$  ppm for the modern tree-rings sampled). Paleoclimate proxies based on certain aspects of plant anatomy or physiological function can potentially be affected by [CO<sub>2</sub>] (Cowling and Sykes 1999) because low [CO<sub>2</sub>] generally increases stomatal conductance and transpiration and therefore increases transport demands imposed on the xylem (Tyree and Alexander 1993). Indeed, gas exchange data for bur oaks sampled at the MO, WI, and SD sites suggest that for net photosynthesis to be equivalent across ambient [CO<sub>2</sub>] at 350 vs. 220 ppm, stomatal conductance would need to increase by  $\sim 40\%$  (i.e.,  $180\text{--}300 \text{ mmol}\cdot\text{m}^{-2}\cdot\text{s}^{-1}$ ) (S. Voelker, unpublished data; leaf temperature range was  $20\text{--}34^\circ\text{C}$  and vapor pressure deficits were non-limiting). Furthermore, stomatal density in oaks and other tree species has been shown to have an inverse relationship with [CO<sub>2</sub>]



PLATE 1. (Left) A canopy co-dominant bur oak growing near the Brule River Boreal Forest State Natural Area in northern Wisconsin (USA). This 50–60-year-old closed canopy forest included occasional bur oaks but was dominated by balsam fir, paper birch, and white spruce. (Center) An old-growth bur oak tree growing among a multi-aged stand in Bear Gulch, Custer State Park, South Dakota. The upland area surrounding oaks was previously a ponderosa pine forest but was severely burned during the 1988 Galena Fire. (Right) This subfossil oak log produced sample MED702 that had  $2\sigma$  confidence level  $^{14}\text{C}$  ages of 13 124 and 13 378 years BP (Intcal09 calibrated). The photo was taken at Medicine Creek in northern Missouri. Note the extant oaks growing near the large cut-bank in the background. Sub-fossil oak logs are often found exposed from cut-banks, or after flood events, the logs may be deposited elsewhere within the stream channel as shown here. Photo credits: left and center, S. L. Voelker; right, R. P. Guyette.

(Woodward 1987), suggesting additional increases in the transpirational flux required to assimilate a given amount of  $\text{CO}_2$  under conditions experienced by subfossil oaks. Provisionally, it can be posited that it would be advantageous if wood conductive efficiency were conserved across  $[\text{CO}_2]$  so as to match maximum transpirational demand. Without conductive efficiency tracking transpirational demand, xylem tensions would increase and the safety factor between the water potential inducing stomatal closure and that inducing runaway embolism in the xylem would tend to be narrower under low  $[\text{CO}_2]$ . Indeed, although  $\text{EW}k_s$  varied with changes in spring temperature, it also rarely exceeded the modern range in  $\text{EW}k_s$  across a substantial and biologically relevant range of  $[\text{CO}_2]$  (Fig. 7a, b).

The few experimental data for hardwoods including oaks have found no consistently reported  $\text{CO}_2$  enrichment effects on vessel size or frequency (Atkinson and Taylor 1996, Gartner et al. 2003, Watanabe et al. 2008, 2010). However, vessel size and frequency have a strong inverse relationship. Although this relationship is not simply related to xylem hydraulic efficiency, all else equal a system of conduits will be more efficient if it is nearer the packing limit or is shifted further down and to the right on a plot of conduit frequency vs. conduit diameter (McCulloh et al. 2010, Zanne et al. 2010). Hence, the interpretation of hydraulic efficiency from these  $\text{CO}_2$  experiments is difficult because vessel sizes and frequencies were always considered separately. Another potential confounding factor is that  $\text{CO}_2$  enrichment tends to increase photosynthetic rates and

augment growth, which may increase vessel diameters for a given stem age. Furthermore we are aware of no investigations of wood anatomy for trees grown at experimentally reduced  $[\text{CO}_2]$ . More observational and experimental data are necessary to judge whether trees modulate their xylem hydraulic efficiency to match  $\text{CO}_2$  effects on transpirational demand.

#### *Comparisons of oak anatomy and deposition with other paleoclimate proxies*

The ice core record from Greenland indicates that the late Quaternary was characterized by a 5–10°C increase in temperatures during the B/A (14.5–12.9 ka) followed by a sudden reversal during the YD (12.9–11.6 ka) and another abrupt warming of ~15°C during the PB (Cuffey et al. 1995, Jouzel et al. 1997). At centennial to millennial scales changes in spring temperatures or the frequency of oak deposition in MO were synchronous with the Greenland NGRIP  $\delta^{18}\text{O}$  record and changes in Cariaco grayscale, a record of upwelling caused by variation in trade wind strength (Fig. 7a, b). Our proxy records also show substantial agreement with some aspects of July temperatures estimated for the Midwest using transfer functions applied to the pollen record (Fig. 7a, c). Indeed other data from upstream of the anomalous cold in the circum-North Atlantic during the YD show evidence of altered atmospheric circulation patterns across Alaska, the Rocky Mountains, and eastern North America (Epstein 1995, Lowell et al. 1999, Shuman et al. 2002, Cole and Arundel 2005, Leavitt et

al. 2006, Wurster et al. 2008, Jiménez-Moreno et al. 2011).

Besides summer temperature estimates (Fig. 7c; Viau et al. 2006), the pollen record can yield many other significant insights on climate and vegetation dynamics during the late Quaternary. The dominant biomes inferred for MO during this period varied between spruce parkland, warm mixed forest, and xerophytic scrub (Williams et al. 2004). Oak pollen at sites in Illinois show stable or increasing patterns during the YD (Gonzales and Grimm 2009, Saunders et al. 2010). However, oak abundance appears to be low enough at the onset of the YD that it may not be possible to discern climatic effects during this time solely from this genus. Unfortunately the inferred vegetation type of spruce, oak, and other species that complemented an anomalous peak in black ash (*Fraxinus nigra* Marsh.) during the late B/A have no direct modern analogs with which to confidently identify a climatic signature. Hence the climate that is most similar to an existing vegetation type may correspond to oak savannah/temperate hardwood/boreal conifer transition forests from northern WI to Saskatchewan and even the Black Hills of SD (Overpeck et al. 1992, Williams et al. 2004, Gonzales and Grimm 2009). The predominance of black ash pollen in sediment cores to the east of MO suggests that during the B/A the climate was much warmer compared to the glacial maximum as well as potentially being wetter than modern conditions (Grimm and Jacobson 2004, Saunders et al. 2010). Modeling efforts that use pollen records from central North America leave much room for interpretation of temperature or precipitation regimes but do tend to agree that the YD had a climate distinct from the B/A and PB (Shane and Anderson 1993, Shuman et al. 2002, Gonzales and Grimm 2009). An abrupt decrease in ash pollen and increase in spruce pollen near the 12.9-ka YD boundary suggests that cooler conditions generally presided over the Midwest to the east of our collection area (Shane and Anderson 1993, Shuman et al. 2002, Saunders et al. 2010). Within the dating accuracy of the proxies, reduction in oak deposition in MO was coeval with pollen-based estimates of reduced summer temperatures across the Midwest at the B/A to YD boundary (Fig. 7c). In contrast to these regional trends, a high-resolution sediment core record from northeastern Illinois suggests warmer temperatures from the B/A were sustained for 400–500 years past the onset of the YD in Greenland and the abrupt changes seen in our records (Gonzales and Grimm 2009, Gonzales et al. 2009). Additional careful data collection and dating will be required to ascertain whether these differences can be attributed to uncertain dating in these proxy records or if changes in atmospheric circulation patterns over the Midwest and Great Plains resulted in increased spatial heterogeneity of climate and resulting vegetation dynamics during this period.

Across western North America and the Great Plains, the soil stratigraphic record and shifts in soil carbon  $\delta^{13}\text{C}$  most likely indicate a prevalence of cooler and wetter spring and summer conditions (Haynes 2008, Nordt et al. 2008). A speleothem record from eastern MO shows substantial reductions in  $\delta^{13}\text{C}$  and  $\delta^{18}\text{O}$  of calcite coeval with the Allerød-YD boundary (Denniston et al. 2001). The authors interpreted these data as a shift from  $\text{C}_4$  grasses toward  $\text{C}_3$  vegetation that was synchronous with a rapid drop in average annual temperatures of  $\sim 4^\circ\text{C}$ . Although this is a greater temperature shift than our proxy record suggests (Fig. 7a), the differences in seasonality among the proxy records could account for the discrepancy. A soil depth profile in western MO that spans the YD showed a strong increase in soil carbon  $\delta^{13}\text{C}$  (Dorale et al. 2010), which is opposite in sign compared to the speleothem record of Denniston et al. (2001). Dorale et al. (2010) inferred this shift to be caused by increased aridity during the YD because of the steep east–west precipitation gradient that currently characterizes this region.

*What caused variation in oak deposition during the Late Quaternary?*

We documented two- to threefold changes in oak depositional frequency across the B/A, YD, and PB periods (Fig. 7c). Although some of this variation is due to a relatively low overall sample size, relevant inferences for climate may still be drawn. Climate could have interacted with animal migration patterns, Clovis hunting, or other trophic interactions to affect bur oak population dynamics during the decline and collapse of Pleistocene megafauna (Fiedel and Haynes 2004, Ripple and Beschta 2007, Gill et al. 2009, Ripple and Van Valkenburgh 2010, Saunders et al. 2010). The timing and interactions among these factors is still debated, and thus we will focus only on the potential for climate to impact bur oak populations by affecting physiology or environmental conditions affecting oak deposition rates.

The calibrated  $^{14}\text{C}$ -dates of anatomical variables used to estimate spring temperatures and  $\text{EW}k_s$  were adjusted earlier in time to account for the difference between the younger cambial ages sampled and the older  $^{14}\text{C}$ -dates of outer rings of each sample. Correlations between spring temperatures or  $\text{EW}k_s$  and NGRIP  $\delta^{18}\text{O}$  decreased with shifts in the dating of these variables earlier or later in time. Besides the earliest portion of the oak record, spring temperatures and  $\text{EW}k_s$  were lowest near the onset of the YD (Fig. 7a, b), which agrees with the pollen-based July temperature estimates over the Midwest (Fig. 7c). These patterns coincide with a much reduced oak deposition during the YD and are coeval with the lowest temperatures from the NGRIP  $\delta^{18}\text{O}$  record (Fig. 7).

The direct impact of low temperatures on oaks is most recognized when regional dieback and mortality events have been caused by late frosts (Millers et al. 1989). During the YD, seasonality in insolation at  $40^\circ\text{N}$  was at

its highest levels since the previous interglacial at ca. 80 ka (Berger and Loutre 1991), which when coupled with shifts in atmospheric circulation, may have contributed to spring temperature conditions not coinciding with photoperiodic constraints on budburst and a resulting increase in the frequency of damaging frost events. Frosts can directly cause mortality in young trees (Aizen and Woodcock 1996) and presumably cause dieback and weaken older ring-porous trees when EW vessels undergo embolism during freeze–thaw cycles (Wang et al. 1992, Sperry et al. 1994, Davis et al. 1999).

The calibrated  $^{14}\text{C}$ -dates of the outer rings of each oak were not shifted according to their ring counts or cambial ages because the outer rings are closest to the deposition date of the tree (within a few decades depending on sapwood degradation). Curiously, however, the correlations of oak deposition increased substantially by shifting these dates earlier in time. The optimal shift of these dates was  $\sim 100$  years for both NGRIP  $\delta^{18}\text{O}$  ( $r = 0.44\text{--}0.53$ ) and Cariaco grayscale ( $r = 0.36\text{--}0.55$ ), while for the July temperature estimates the shift was  $\sim 250$  years ( $r = 0.42\text{--}0.65$ ). The range for the length of this shift in the optimal dating corresponds to an average of one to two generations of mature trees given that the mean age of trees sampled was  $\sim 150$  years. If the abundance or viability of seed or the establishment of young oaks is impacted more than older oaks it could help explain the generational lag between the  $^{14}\text{C}$ -dates of oak deposition and other paleoclimate proxies. Under a colder climatic regime promoting a lengthier period of dormancy, the time from a threshold dehardening temperature to budburst and leaf expansion would tend to decrease (Heide 1993, Morin et al. 2010). A more rapid progression from dehardening through leaf expansion during early spring conditions could expose young shoots to an increased likelihood of frost damage. Frost damage may affect young bur oaks to a greater extent because their date of budburst tends to be earlier than mature trees (Augspurger and Bartlett 2003). Moreover, acorn size and total production is reduced by low spring temperatures (Sork et al. 1993, Koenig et al. 1996, Koenig et al. 2009) and freezing or low temperatures may more strongly affect young trees (Voelker 2011) or those from small acorns produced at the northern edge of the range (Aizen and Woodcock 1996).

The deposition of bur oaks was much lower during the YD compared with the mean deposition rate across the rest of the oak record investigated here, which suggests oak populations may have been diminished in association with low temperatures (Fig. 7c). However, the number of trees deposited and buried in alluvial sediments may have been less if dry conditions prevailed over this region during the YD and less frequent flooding resulted in either of stream aggradation or a reduction in channel movement compared to that which has characterized these streams during modern times (Guyette et al. 2008). Evidence for increased aridity

during the YD is sparse (but see Dorale et al. 2010); however droughts more severe than the Dust Bowl have occurred within this region within the past 1000 years (Stambaugh et al. 2011). Subfossil wood recovered thus far from conifer species that are usually present in sub-boreal and boreal forests has all dated to before the YD (R. Guyette, *unpublished data*; D. Grimley, *personal communication*). This negative evidence for conifer occurrence during the YD may again indicate reduced channel movement or that YD climate favored grass, shrub, or hardwood species that we did not sample. Hence, despite knowledge that low temperatures can reduce the establishment and survival of modern oaks and that temperature variation impacted paleo bur oak physiology, the unknown rates of channel movement and species composition prevent the attribution of changes in oak deposition solely to temperature effects on oak populations.

#### *Mechanisms for climate change over the American mid-continent*

Many proxies indicate climate changed rapidly over North America following the collapse of the North Atlantic thermohaline cycle and the onset of the YD. These changes are thought to have been driven by an eastward shift in the Aleutian low and advection of Siberian air over the North Pacific with eventual transport of these cold and dry winter air masses to the American mid-continent (Mikolajewicz et al. 1997, Yu and Wright 2001, Okumura et al. 2009). There is evidence of a high pressure system over the southern Laurentide ice sheet that produced anticyclonic winds during the ice-free season for the northern Great Lakes region (Krist and Schaetzl 2001). The location of such a high pressure system, in conjunction with ice sheet topography and the Coriolis force would have acted to deflect zonal air flow to the south. As a result, a reduction in pressure gradients between the Gulf of Mexico and the Midwest would have dampened the diurnal oscillation that drives low-level jet nocturnal transport of warm and moist air northward from the Gulf of Mexico during the spring and summer (Higgins et al. 1997, Mo et al. 1997, Ting and Wang 2006). This sequence of effects could promote clear conditions and cold nighttime spring temperatures (i.e., an increased likelihood of late frosts) considering the increased seasonality of this period (Berger and Loutre 1991).

In a separate but related scenario the pressure difference that defines the North Atlantic Oscillation would have been reduced during the YD, triggering a southward shift of the intertropical convergence zone (ITCZ) and increased trade wind strength. Consistent with this interpretation, patterns in Cariaco grayscale indicate increased upwelling and drier conditions along the northern coast of South America (Hughen et al. 1996, 2000). A southerly shift in the ITCZ could have induced a more zonal flow for the easterly trade winds across the Caribbean, which tends to characterize wind

flow during dry conditions over the Great Plains (Mo and Berbery 2004). Yet, as Gonzales and Grimm (2009) suggest, zonal air masses colliding with cold air currents near the Laurentide ice sheet may have yielded locally wet conditions in the upper Midwest. Thereby, a stronger moisture gradient between the Great Plains and the Midwest than is currently observed may explain the differences in interpretation of a cool and/or wet YD climate in eastern MO and much of the Midwest (Denniston et al. 2001, Shuman et al. 2002, Viau et al. 2006, Gonzales et al. 2009) and a drier YD in southwestern MO by Dorale et al. (2010).

## ACKNOWLEDGMENTS

We thank the numerous student workers for helping process samples and the private landowners who granted us permission to access subfossil wood samples. We appreciate the technical assistance provided by Lara Läubli. We also thank Gary Brundige for permission to collect samples at Custer State Park. Eric Grimm and one anonymous reviewer provided valuable comments and insight that improved this manuscript. This research was supported by the National Science Foundation grant nos. DEB-0743882 and ATM-0601884.

## LITERATURE CITED

- Ahlgren, C. E. 1957. Phenological observations of nineteen native tree species in northeastern Minnesota. *Ecology* 38:622–628.
- Aizen, M. A., and H. Woodcock. 1996. Effects of acorn size on seedling survival and growth in *Quercus rubra* following simulated freeze. *Canadian Journal of Botany* 74:308–314.
- Alley, R. B. 2000. The Younger Dryas cold interval as viewed from central Greenland. *Quaternary Science Reviews* 19:213–226.
- Alves, G., M. Decourteix, P. Fleurat-Lessard, S. Sakr, M. Bonhomme, T. Ameglio, A. Lacoïnte, J. L. Julien, G. Petel, and A. Guilliot. 2007. Spatial activity and expression of plasma membrane H(+)-ATPase in stem xylem of walnut during dormancy and growth resumption. *Tree Physiology* 27:1471–1480.
- Atkinson, C. J., and M. P. Denne. 1988. Reactivation of vessel production in ash (*Fraxinus excelsior*) trees. *Annals of Botany* 61:679–688.
- Atkinson, C. J., and J. M. Taylor. 1996. Effects of elevated CO<sub>2</sub> on stem growth, vessel area and hydraulic conductivity of oak and cherry seedlings. *New Phytologist* 133:617–626.
- Augsperger, C. K., and E. A. Bartlett. 2003. Differences in leaf phenology between juvenile and adult trees in a temperate forest. *Tree Physiology* 23:517–525.
- Bansal, S., and M. J. Germino. 2008. Carbon balance of conifer seedlings at timberline: relative changes in uptake, storage, and utilization. *Oecologia* 158:217–227.
- Becker, B. 1993. An 11,000-year German oak and pine dendrochronology for radiocarbon calibration. *Radiocarbon* 35:201–213.
- Bell, D. T., and F. L. Johnson. 1975. Phenological patterns in the trees of the streamside forest. *Bulletin of the Torrey Botanical Club* 102:187–193.
- Berger, A., and M. F. Loutre. 1991. Insolation values for the climate of the last 10 million years. *Quaternary Sciences Review* 10:297–317.
- Bonhomme, M., M. Peuch, T. Ameglio, R. Rageu, A. Guilliot, M. Decourteix, G. Alves, S. Sakr, and A. Lacoïnte. 2009. Carbohydrate uptake from xylem vessels and its distribution among stem tissues and buds in walnut (*Juglans regia* L.). *Tree Physiology* 30:89–102.
- Briffa, K. R., and T. M. Melvin. 2008. A closer look at regional curve standardization of tree-ring records: justification of the need, a warning of some pitfalls and suggested improvements in its application. Pages 113–145 in M. K. Hughes, T. W. Swetnam, and H. F. Diaz, editors. *Dendroclimatology: progress and prospects*. Springer, New York, New York, USA.
- Briffa, K. R., T. J. Osborn, F. H. Schweingruber, I. C. Harris, P. D. Jones, S. G. Shiyatov, and E. A. Vaganov. 2001. Low-frequency temperature variations from a northern tree ring density network. *Journal of Geophysical Research* 106:2929–2941.
- Brown, A. G. 1997. *Alluvial geoarchaeology: floodplain archaeology and environmental change*. Cambridge University Press, Cambridge, UK.
- Burns, R. M., and B. H. Honkala. 1990. *Silvics of North America: 1. Conifers; 2. Hardwoods*. Agriculture Handbook 654. USDA Forest Service, Washington, D.C., USA.
- Carlson, A. E. 2010. What caused the Younger Dryas cold event? *Geology* 38:383–384.
- Carlson, A. E., P. U. Clark, B. A. Haley, G. P. Klinkhamer, K. Simmons, E. J. Brook, and K. Meissner. 2007. Geochemical proxies of North American freshwater routing during the Younger Dryas cold event. *Proceedings of the National Academy of Sciences USA* 104:6556–6561.
- Cole, K. L., and S. T. Arundel. 2005. Carbon isotopes from fossil packrat pellets and elevational movements of Utah agave plants reveal the Younger Dryas cold period in Grand Canyon, Arizona. *Geology* 33:713–716.
- Cowling, S. A., and M. T. Sykes. 1999. Physiological significance of low atmospheric CO<sub>2</sub> for plant–climate interactions. *Quaternary Research* 52:237–242.
- Cuffey, K. M., G. D. Clow, R. B. Alley, M. Stuiver, E. D. Waddington, and R. W. Saltus. 1995. Large arctic temperature change at the Wisconsin–Holocene glacial transition. *Science* 270:455–458.
- Davis, S. D., J. S. Sperry, and U. G. Hacke. 1999. The relationship between xylem conduit diameter and cavitation caused by freezing. *American Journal of Botany* 86:1367–1372.
- Denniston, R. F., L. A. González, Y. Asmerom, V. Polyak, M. K. Reagan, and M. R. Saltzman. 2001. A high-resolution speleothem record of climatic variability during the Allerød–Younger Dryas transition in Missouri, central United States. *Palaeogeography, Palaeoecology, Palaeoclimatology* 176:147–155.
- Dorale, J. A., L. A. Wozniak, E. A. Bettis, S. J. Carpenter, R. D. Mandel, E. R. Hajic, N. H. Lopinot, and J. H. Ray. 2010. Isotopic evidence for Younger-Dryas aridity in the North American midcontinent. *Geology* 38:519–522.
- Dougherty, P. M., R. O. Teskey, J. E. Helps, and T. M. Hinckley. 1979. Net photosynthesis and early growth trends of a dominant white oak (*Quercus alba* L.). *Plant Physiology* 64:930–935.
- Edwards, N. T., and P. J. Hanson. 1996. Stem respiration in a closed-canopy upland oak forest. *Tree Physiology* 16:433–439.
- Eilmann, B., P. Weber, A. Rigling, and D. Eckstein. 2006. Growth reactions of *Pinus sylvestris* L. and *Quercus pubescens* Willd. to drought years at a xeric site in Valais, Switzerland. *Dendrochronologia* 23:121–132.
- Epstein, S. 1995. The isotopic climatic records in the Allerød–Bölling–Younger Dryas and post-Younger Dryas events. *Global Biogeochemical Cycles* 9:557–563.
- Esper, J., E. R. Cook, and F. H. Schweingruber. 2002. Low-frequency signals in long tree-ring chronologies for reconstructing past temperature variability. *Science* 295:2250–2253.
- Fiedel, S., and G. Haynes. 2004. A premature burial: comments on Grayson and Meltzer’s “Requiem for overkill.” *Journal of Archaeological Science* 31:121–131.
- Fonti, P., and I. García-González. 2008. Earlywood vessel size of oak as a potential proxy for spring precipitation in mesic sites. *Journal of Biogeography* 35:2249–2257.

- Fonti, P., N. Solomonoff, and I. García-González. 2007. Earlywood vessels of *Castanea sativa* record temperature before their formation. *New Phytologist* 163:562–570.
- Fonti, P., G. von Arx, I. García-González, B. Eilmann, U. Sass-Klassen, H. Gärtner, and D. Eckstein. 2010. Studying global change through investigation of the plastic response of xylem anatomy in tree rings. *New Phytologist* 185:42–53.
- Frankenstein, C., D. Eckstein, and U. Schmitt. 2005. The onset of cambium activity—A matter of agreement? *Dendrochronologia* 23:57–62.
- Friedrich, M., S. Remmele, B. Kromer, J. Hofmann, M. Spurk, K. F. Kaiser, C. Orzel, and M. Küppers. 2004. The 12,460-year Hohenheim oak and pine tree-ring chronology from central Europe; a unique annual record for radiocarbon calibration and paleoenvironment reconstructions. *Radiocarbon* 46:1111–1122.
- García-González, I., and D. Eckstein. 2003. Climatic signal of earlywood vessels of oak on a maritime site. *Tree Physiology* 23:497–504.
- Gartner, B. L., J. Roy, and R. Huc. 2003. Effects of tension wood on specific conductivity and vulnerability to embolism of *Quercus ilex* seedlings grown at two atmospheric CO<sub>2</sub> concentrations. *Tree Physiology* 23:387–395.
- Gill, J. L., J. L. Williams, S. T. Jackson, K. B. Lininger, and G. S. Robinson. 2009. Pleistocene megafaunal collapse, novel plant communities, and enhanced fire regimes in North America. *Science* 326:1100–1103.
- Gonzales, L. M., and E. C. Grimm. 2009. Synchronization of late-glacial vegetation changes at Crystal Lake, Illinois, USA with the North Atlantic event stratigraphy. *Quaternary Research* 72:234–245.
- Gonzales, L. M., J. W. Williams, and E. C. Grimm. 2009. Expanded response surfaces: a new method to reconstruct paleoclimates from fossil pollen assemblages that lack modern analogues. *Quaternary Science Reviews* 28:3315–3332.
- Grimm, E. C. 2000. North American pollen database. World Data Center for Paleoclimatology, Asheville, North Carolina, USA. <http://www.ncdc.noaa.gov/paleo/napd.html>
- Grimm, E. C., and G. L. Jacobson, Jr. 2004. Late Quaternary vegetation history of the eastern United States. Pages 381–402 in A. R. Gillespie, S. C. Porter, and B. F. Atwater, editors. *The Quaternary period in the United States*. Elsevier, Boston, Massachusetts, USA.
- Grissino-Mayer, H. D. 2001. Evaluating crossdating accuracy: a manual and tutorial for the computer program COFECHA. *Tree-Ring Research* 57:205–221.
- Guyette, R. P., D. C. Dey, and M. C. Stambaugh. 2008. The temporal distribution and carbon storage of large oak wood in streams and floodplain deposits. *Ecosystems* 11:643–653.
- Guyette, R. P., and M. C. Stambaugh. 2003. The age and density of ancient and modern oak wood in streams and sediments. *International Association of Wood Anatomists Journal* 24:345–353.
- Haynes, C. V., Jr. 2008. Younger Dryas “black mats” and the Rancholabrean termination in North America. *Proceedings of the National Academy of Sciences USA* 105:6520–6525.
- Heide, O. M. 1993. Daylength and thermal time responses of budburst during dormancy release in some northern deciduous trees. *Physiologia Plantarum* 88:531–540.
- Higgins, R. W., Y. Yao, E. S. Yarosh, J. E. Janowiak, and K. C. Mo. 1997. Influence of Great Plains low-level jet on summertime precipitation and moisture transport over the central United States. *Journal of Climate* 10:481–507.
- Hoch, G., and C. Körner. 2009. Growth and carbon relations of tree line forming conifers at constant vs. variable low temperatures. *Journal of Ecology* 97:57–66.
- Holmes, R. L. 1983. Computer-assisted quality control in tree-ring dating and measurement. *Tree-Ring Bulletin* 43:69–78.
- Hughen, K. A., J. T. Overpeck, L. C. Peterson, and S. Trumbore. 1996. Rapid climate changes in the tropical Atlantic region during the last deglaciation. *Nature* 380:51–54.
- Hughen, K. A., J. R. Southon, S. J. Lehman, and J. T. Overpeck. 2000. Synchronous radiocarbon and climate shifts during the last deglaciation. *Science* 290:1951–1954.
- Jiménez-Moreno, G., R. S. Anderson, V. Atudorei, and J. L. Toney. 2011. A high-resolution record of climate, vegetation, and fire in the mixed conifer forest of northern Colorado, USA. *Geological Society of America Bulletin* 123:240–254.
- Johnsen, K., C. Maier, F. Sanchez, P. Anderson, J. Butnor, R. Waring, and S. Linder. 2007. Physiological girdling of pine trees via phloem chilling: proof of concept. *Plant, Cell and Environment* 30:128–134.
- Jouzel, J., et al. 1997. Validity of the temperature reconstruction from water isotopes in ice cores. *Journal of Geophysical Research* 102:26,471–26,487.
- Koenig, W. D., J. M. H. Knops, W. J. Carmen, M. T. Stanback, and R. L. Mumme. 1996. Acorn production by oaks in central coastal California: influence of weather at three levels. *Canadian Journal of Forest Research* 26:1677–1683.
- Koenig, W. D., J. M. H. Knops, J. L. Dickinson, and B. Zuckerman. 2009. Latitudinal decrease in acorn size in bur oak (*Quercus macrocarpa*) is due to environmental constraints, not avian dispersal. *Canadian Journal of Botany* 87:349–356.
- Körner, C., and G. Hoch. 2006. A test of treeline theory on a montane permafrost island. *Arctic, Antarctic, and Alpine Research* 38:113–119.
- Krist, F., and R. J. Schaetzl. 2001. Paleowind (11,000 BP) directions derived from lake spits in Northern Michigan. *Geomorphology* 38:1–18.
- Kromer, B., and M. Spurk. 1998. Revision and tentative extension of the tree-ring based <sup>14</sup>C calibration, 9200 to 11,855 cal BP. *Radiocarbon* 40:1117–1125.
- Lachenbruch, B., J. R. Moore, and R. Evans. 2011. Radial variation in wood structure and function in woody plants, and hypotheses for its occurrence. Pages 121–164 in F. C. Meinzer, B. Lachenbruch, and T. E. Dawson, editors. *Size and age-related changes in tree structure and function*. Springer, New York, New York, USA.
- Leavitt, S. W., I. P. Panyushkina, T. Lange, A. Wiedenhoef, L. Cheng, R. D. Hunter, J. Hughes, F. Pranschke, A. F. Schneider, J. Moran, and R. Stieglitz. 2006. Climate in the Great Lakes region between 14,000 and 4000 years ago from isotopic composition of conifer wood. *Radiocarbon* 48:205–217.
- Leopold, A., and S. E. Jones. 1947. A phenological record for Sauk and Dane counties, Wisconsin, 1935–1945. *Ecological Monographs* 17:81–122.
- Lowell, T. V., G. J. Larson, J. D. Hughes, and G. H. Denton. 1999. Age verification of the Lake Gribben forest bed and the Younger Dryas advance of the Laurentide ice sheet. *Canadian Journal of Earth Science* 36:383–393.
- Mann, M. E., R. S. Bradley, and M. K. Hughes. 1999. Northern hemisphere temperatures during the past millennium: inferences, uncertainties, and limitations. *Geophysical Research Letters* 26:759–762.
- McCulloh, K., J. S. Sperry, B. Lachenbruch, F. C. Meinzer, P. B. Reich, and S. Voelker. 2010. Moving water well: comparing hydraulic efficiency in twigs and trunks of coniferous, ring-porous, and diffuse-porous saplings from temperate and tropical forests. *New Phytologist* 186:439–450.
- Mikolajewicz, U., T. J. Crowley, A. Schiller, and R. Voss. 1997. Modeling North Atlantic/North Pacific teleconnections during the Younger Dryas. *Nature* 387:384–387.
- Millers, I., D. S. Shriner, and D. Rizzo. 1989. History of hardwood decline in the Eastern United States. USDA Forest Service General Technical Report NE-126.

- Mo, K. C., and E. H. Berbery. 2004. Low-level jets and the summer precipitation regimes over North America. *Journal of Geophysical Research Atmospheres* 109:D06117.
- Mo, K. C., J. N. Paegler, and R. W. Higgins. 1997. Atmospheric processes associated with summer floods and droughts in the central United States. *Journal of Climate* 10:3028–3046.
- Moberg, A., D. M. Sonechkin, K. Holmgren, N. M. Datsenko, and W. Karlen. 2005. Highly variable Northern Hemisphere temperatures reconstructed from low- and high-resolution proxy data. *Nature* 433:613–617.
- Morin, X., J. Roy, L. Sonié, and I. Chuine. 2010. Changes in phenology of three European oak species in response to experimental climate change. *New Phytologist* 186:900–910.
- Mu, Q., F. A. Heinsch, M. Zhao, and S. W. Running. 2007. Development of a global evapotranspiration algorithm based on MODIS and global meteorology data. *Remote Sensing of Environment* 111:519–536.
- Mu, Q., L. A. Jones, J. S. Kimball, K. C. McDonald, and S. W. Running. 2009. Satellite assessment of land surface evapotranspiration for the pan-Arctic domain. *Water Resources Research* 45:W09420.
- NGRIP members (North Greenland Ice Core Project). 2004. High-resolution record of Northern Hemisphere climate extending into the last interglacial period. *Nature* 431:147–151.
- Nilsson, T., and G. Daniel. 1990. Structure and the aging process of dry archaeological wood. Pages 67–86 in R. M. Rowell and R. J. Barbour, editors. *Archaeological wood*. American Chemical Society, Washington, D.C., USA.
- Nordt, L., J. von Fischer, L. Tieszen, and J. Tubbs. 2008. Coherent changes in relative C<sub>4</sub> plant productivity and climate during the late Quaternary in the North American Great Plains. *Quaternary Science Reviews* 27:1600–1611.
- Okumura, Y. M., C. Deser, A. Hu, A. Timmermann, and S.-P. Xie. 2009. North Pacific climate response to freshwater forcing in the subarctic North Atlantic: oceanic and atmospheric pathways. *Journal of Climate* 22:1424–1445.
- Overpeck, J. T., R. S. Webb, and T. Webb III. 1992. Mapping eastern North American vegetation change of the past 18 ka: no-analogs and the future. *Geology* 20:1071–1074.
- Peteet, D. M., A. Del Genio, and K. K.-W. Lo. 1997. Sensitivity of northern hemisphere air temperatures and snow expansion to North Pacific sea surface temperatures in the Goddard Institute for Space Studies general circulation model. *Journal of Geophysical Research* 102:23781–23791.
- Reimer, P. J., et al. 2009. IntCal09 and Marine09 radiocarbon age calibration curves 0–50,000 years cal BP. *Radiocarbon* 51:1111–1150.
- Ripple, W. J., and R. L. Beschta. 2007. Hardwood tree decline following large carnivore loss on the Great Plains, USA. *Frontiers in Ecology and the Environment* 5:241–246.
- Ripple, W. J., and B. Van Valkenburgh. 2010. Linking top-down forces to the Pleistocene megafaunal extinctions. *BioScience* 60:516–526.
- Saunders, J. J., E. C. Grimm, C. C. Widga, G. D. Campbell, B. B. Curry, D. A. Grimley, P. R. Hanson, J. P. McCullum, J. S. Oliver, and J. D. Treworgy. 2010. Paradigms and proboscideans in the southern Great Lakes region, USA. *Quaternary International* 217:175–187.
- Schniewind, A. P. 1990. Physical and mechanical properties of archaeological wood. Pages 87–110 in R. M. Rowell and R. J. Barbour, editors. *Archaeological wood*. American Chemical Society, Washington, D.C., USA.
- Schrader, J., K. Baba, S. T. May, K. Palme, M. Bennett, R. P. Bhalerao, and G. Sandberg. 2003. Polar auxin transport in the wood-forming tissues of hybrid aspen is under simultaneous control of developmental and environmental signals. *Proceedings of the National Academy of Sciences USA* 100:10096–10101.
- Shane, L. C. K., and K. H. Anderson. 1993. Intensity, gradients and reversals in late glacial environmental change in east-central north America. *Quaternary Science Reviews* 12:307–320.
- Shuman, B. N., T. Webb III, P. J. Bartlein, and J. W. Williams. 2002. The anatomy of a climatic oscillation: vegetation change in eastern North America during the Younger Dryas chronozone. *Quaternary Science Reviews* 21:1777–1791.
- Sieg, C. H., D. M. Meko, A. D. DeGaetano, and W. Ni. 1996. Dendroclimatic potential in the northern Great Plains. Pages 295–302 in J. S. Dean, D. M. Meko, and T. W. Swetnam, editors. *Tree rings, environment and humanity*. Proceedings of the International Conference. Radiocarbon, Tucson, Arizona, USA.
- Sork, V. L., J. Bramble, and O. Sexton. 1993. Ecology of mast-fruiting in three species of North American deciduous oaks. *Ecology* 74:528–541.
- Speer, J., H. D. Grissino-Mayer, K. H. Orvis, and C. H. Greenberg. 2009. Climate response of five oak species in the eastern deciduous forest of the southern Appalachian Mountains, USA. *Canadian Journal of Forest Research* 39:507–518.
- Sperry, J. S., and T. Ikeda. 1997. Xylem cavitation in roots and stems of Douglas-fir and white fir. *Tree Physiology* 17:275–280.
- Sperry, J. S., K. L. Nichols, J. E. M. Sullivan, and S. E. Eastlack. 1994. Xylem embolism in ring-porous, diffuse-porous, and coniferous trees of northern Utah and interior Alaska. *Ecology* 75:1736–1752.
- Spurk, M., H. H. Leuschner, M. G. L. Baillie, K. R. Briffa, and M. Friedrich. 2002. Depositional frequency of German subfossil oaks: climatically and non-climatically induced fluctuations in the Holocene. *Holocene* 12:707–715.
- Stahle, D. W., and J. G. Hehr. 1984. Dendroclimatic relationships of post oak across a precipitation gradient in the southcentral United States. *Annals of the Association of American Geographers* 74:561–573.
- Stambaugh, M. C., and R. P. Guyette. 2009. Progress in constructing a long oak chronology from the central United States. *Tree-Ring Research* 65:147–156.
- Stambaugh, M. C., R. P. Guyette, E. R. McMurphy, E. R. Cook, D. M. Meko, and A. C. Lupo. 2011. Drought duration and frequency in the U.S. Corn Belt during the last millennium (AD 992–2004). *Agricultural Forest Meteorology* 151:154–162.
- St. George, S., and E. Nielsen. 2002. Hydroclimatic change in southern Manitoba since A.D. 1409 inferred from tree rings. *Quaternary Research* 58:103–111.
- Stuiver, M., and P. J. Reimer. 1993. Extended <sup>14</sup>C data base and revised CALIB 3.0 <sup>14</sup>C age calibration program. *Radiocarbon* 35:215–230.
- Susiloto, S., E. Hilavuori, and F. Berninger. 2010. Testing the growth limitation hypothesis for subarctic Scots pine. *Journal of Ecology* 98:1186–1195.
- Sveinbjörnsson, B., M. Smith, T. Traustason, R. W. Ruess, and P. F. Sullivan. 2010. Variation in carbohydrate source–sink relations of forest and treeline white spruce in southern, interior and northern Alaska. *Oecologia* 163:833–843.
- Ting, M., and H. Wang. 2006. The role of the North American topography on the maintenance of the Great Plains summer low-level jet. *Journal of the Atmospheric Sciences* 63:1056–1068.
- Tyree, M. T., and J. D. Alexander. 1993. Plant water relations and the effects of elevated CO<sub>2</sub>: a review and suggestions for future research. *Vegetatio* 104/105:47–62.
- Viau, A. E., K. Gajewski, M. C. Sawada, and P. Fines. 2006. Millennial-scale temperature variations in North America during the Holocene. *Journal of Geophysical Research* 111:D09102.
- Voelker, S. L. 2011. Age-dependent changes in environmental influences on tree growth and their implications for forest responses to climate change. Pages 455–479 in F. C. Meinzer, B. Lachenbruch, and T. E. Dawson, editors. *Size and age-*

- related changes in tree structure and function. Springer, New York, New York, USA.
- Wang, J., D. E. Ives, and M. J. Lechowicz. 1992. The relation of foliar phenology to xylem embolism in trees. *Functional Ecology* 4:469–475.
- Warton, D. I., I. J. Wright, D. S. Falster, and M. Westoby. 2006. Bivariate line-fitting methods for allometry. *Biological Reviews* 81:259–291.
- Watanabe, Y., T. Satomura, K. Sasa, R. Funada, and T. Koike. 2010. Differential anatomical responses to elevated CO<sub>2</sub> in saplings of four hardwood species. *Plant, Cell and Environment* 33:1101–1111.
- Watanabe, Y., H. Tobita, M. Kitao, Y. Maruyama, D. Choi, K. Sasa, R. Funada, and T. Koike. 2008. Effects of elevated CO<sub>2</sub> and nitrogen on wood structure related to water transport in seedlings of two deciduous broad-leaved tree species. *Trees* 22:403–411.
- Way, D. A., and R. Oren. 2010. Differential responses to changes in growth temperature between trees from differential functional groups and biomes: a review and synthesis of data. *Tree Physiology* 30:669–688.
- White, P. B., S. L. van de Gevel, H. D. Grissino-Mayer, L. B. LaForest, and G. D. Deweese. 2010. Climatic response of oak species across an environmental gradient in the southern Appalachian Mountains, USA. *Tree-Ring Research* 67:27–37.
- Williams, J. W., B. N. Shuman, T. Webb III, P. J. Bartlein, and P. Leduc. 2004. Quaternary vegetation dynamics in North America: scaling from taxa to biomes. *Ecological Monographs* 74:309–334.
- Woodward, I. F. 1987. Stomatal numbers are sensitive to increases in CO<sub>2</sub> from pre-industrial levels. *Nature* 327:617–618.
- Wurster, C. M., W. P. Patterson, D. A. McFarlane, L. I. Wassenaar, K. A. Hobson, N. B. Athfield, and M. I. Bird. 2008. Stable carbon and hydrogen isotopes from bat guano in the Grand Canyon, USA, reveal Younger Dryas and 8.2 ka events. *Geology* 36:683–686.
- Yu, Z., and H. E. Wright. 2001. Response of interior North America to abrupt climate oscillations in the North Atlantic region during the last deglaciation. *Earth-Science Reviews* 52:333–369.
- Zanne, A. E., M. Westoby, D. S. Falster, D. D. Ackerly, S. R. Loarie, S. E. J. Arnold, and D. A. Coomes. 2010. Angiosperm wood structure: global patterns in vessel anatomy and its relationship to wood density and potential conductivity. *American Journal of Botany* 97:207–215.
- Zasada, J. C., and R. Zahner. 1969. Vessel element development in the earlywood of red oak (*Quercus rubra*). *Canadian Journal of Botany* 47:1965–1971.

#### SUPPLEMENTAL MATERIAL

##### Appendix

Supporting descriptions of methods and results (*Ecological Archives* M082-006-A1).

##### Supplement

Radiocarbon dates, laboratories, errors in dating, and associated anatomical measurements from subfossil oaks (*Ecological Archives* M082-066-S1).